Submitted to Physical Review

UCRL-19539
preprint

c.2

RECEIVED
LAWRENCE
RADIATION LABORATORY
MAY 15 1970
LIBRARY AND
DOCUMENTS SECTION

PRODUCTION AND DECAY PROPERTIES OF PROTACTINIUM ISOTOPES OF MASS 222 TO 225 FORMED IN HEAVY ION REACTIONS

Jørn Borggreen, Kalevi Valli, and Earl K. Hyde

February 1970

AEC Contract No. W-7405-eng-48

TWO-WEEK LOAN COPY

This is a Library Circulating Copy which may be borrowed for two weeks. For a personal retention copy, call Tech. Info. Division, Ext. 5545

UCRL-19539

LAWRENCE RADIATION LABORATORY
UNIVERSITY of CALIFORNIA BERKELEY

DISCLAIMER

This document was prepared as an account of work sponsored by the United States Government. While this document is believed to contain correct information, neither the United States Government nor any agency thereof, nor the Regents of the University of California, nor any of their employees, makes any warranty, express or implied, or assumes any legal responsibility for the accuracy, completeness, or usefulness of any information, apparatus, product, or process disclosed, or represents that its use would not infringe privately owned rights. Reference herein to any specific commercial product, process, or service by its trade name, trademark, manufacturer, or otherwise, does not necessarily constitute or imply its endorsement, recommendation, or favoring by the United States Government or any agency thereof, or the Regents of the University of California. The views and opinions of authors expressed herein do not necessarily state or reflect those of the United States Government or any agency thereof or the Regents of the University of California.

PRODUCTION AND DECAY PROPERTIES OF PROTACTINIUM ISOTOPES OF MASS 222 TO 225 FORMED IN HEAVY ION REACTIONS*

Jørn Borggreen†, Kalevi Valli††, and Earl K. Hyde

Nuclear Chemistry Division
Lawrence Radiation Laboratory
University of California
Berkeley, California 94720

February 1970

ABSTRACT

Four alpha-decay chains initiated by ^{225}Pa, ^{224}Pa, ^{223}Pa, and ^{222}Pa were produced by the bombardment of thallium, lead, and bismuth targets with beams of ^{22}Ne, ^{20}Ne, ^{19}F, ^{18}O, ^{16}O, ^{15}N, and ^{14}N at the Berkeley HILAC. The reaction products were transported from the reaction cell by the helium jet technique and their decay measured with a semiconductor detector. Energy values, excitation functions, half lives, and genetic relationships of individual peaks were determined. Two new techniques based on the use of a time-to-amplitude converter were developed for the measurement of microsecond half lives of daughter products and 5 half lives in the microsecond range were measured.

These new alpha data help to determine the trends in alpha-decay energies for isotopes of odd-Z elements, particularly in the poorly-defined region just above the 126 neutron shell. This allows more accurate predictions of alpha-decay properties of many unknown nuclei. Some anomalous behavior of the apparent alpha-decay energies for nuclei with 133 and 135 neutrons is pointed out.

I. INTRODUCTION

In a recent paper[1] we have presented new information on thorium isotopes of mass 221 to 224 and on the radium and radon isotopes into which they decay. These nuclides fall in that part of the nuclide chart just above the 82 proton and 126 neutron shells where nuclear information has been sparse because of the instability of the nuclei and the difficulty of making them. Reactions induced by complex nuclear projectiles such as ^{14}N, ^{16}O, ^{19}F, ^{20}Ne and ^{22}Ne in such targets as thallium, lead, and bismuth provide one means of reaching this region of the nuclide chart. The previous paper was restricted to a study of nuclides of even atomic number prepared by such reactions. In the present paper we discuss results on odd-Z products, specifically the alpha decay chains initiated by ^{225}Pa, ^{224}Pa, ^{223}Pa and ^{222}Pa. Figure 1 shows the four series about which new information was obtained in this study and shows their location in the Chart of the Nuclides.

This study was conducted because of the intrinsic interest in the decay properties of unknown nuclei, particularly those far from beta stability. Such alpha decay data are also useful for making estimates of ground state masses, for testing the predictions of atomic mass equations and prescriptions, and for other matters related to the systematic trends in ground state properties.

An additional reason for this study is the need for background information for a proper interpretation of alpha data obtained in nuclear reactions involving transuranium element targets. There is an intense interest in reactions which provide information on nuclides of charge greater than 100. But the desired products of such reactions typically have cross sections far below the microbarn level with the result that there can

be serious interference in the observed alpha spectra from alpha emitting isotopes of much lower nuclear charge produced in reactions induced in target impurities or by unusual partial transfer or nuclear break-up reactions. It is important that complete information be available on these possible contaminants particularly those with alpha particle energies greater than $\sim$ 9 MeV.

In this work targets of ^{205}Tl, ^{206}Pb, ^{208}Pb and ^{209}Bi were bombarded with heavy ion beams from the Berkeley Heavy Ion Linear Accelerator (HILAC). Thin targets were used and the recoiling products of the nuclear reactions were slowed down in a helium atmosphere and then transported by a helium gas stream through a capillary of several centimeters length to an evacuated counting chamber where they were deposited on a metal surface positioned in front of a gold surface-barrier detector which was used to measure the alpha radiations emitted by the collected sample. Recent developments in our experimental technique which permit us to collect and study nuclides with half lives as short as 1 msec are discussed in our previous publications.[1,2,3] Similar developments have been reported by R. D. MacFarlane and his associates.[4]

We studied the products from 14 combinations of target and projectile (see Table I) and for each combination performed measurements at several beam energies. For each case the energies and relative abundances of the alpha particles were measured and changes in these were noted as a function of bombardment energy. We used several techniques to determine the half lives of specific alpha particle groups and to establish the genetic relationship of one activity to another. A combination of arguments was used to determine the assignment of all observed alpha groups to specific nuclides.

One important aid in the preliminary assignment of the alpha groups was Fig. 2 which is a plot of the systematic trends in the alpha particle energy for ground state decay when isotopes of a specific element are plotted against neutron number. This plot, including its sharp discontinuity at the 126 neutron shell, is well-known but up until this work there were not enough data for the isotopes of Pa, Ac, and Fr in the 127-135 neutron region to extrapolate the curves with much confidence. In Fig. 2 points taken from the literature are shown as black dots while experimental points based on the assignments of the present study are given as triangles. In the decay of odd-Z nuclides, particularly those of odd-odd type the favored decay is not usually to the ground state so there can be uncertainty in the value to be taken for the ground-state transition. Such cases are indicated by upward-directed arrows. A similar curve for even-Z nuclides is given in our previous paper.[1]

In Sec. II we discuss those details of our experimental methods which differ from those described in our past publications. In particular we describe some new techniques in Sec. II E which permitted us to measure half lives of microsecond daughter activities. Section III presents the experimental data and the detailed arguments upon which the conclusions are based. A concise summary of all new information from this study is given in Table II. Some discussion of the results is given in Sec. IV.

II. EXPERIMENTAL

Many of the details of our experimental techniques are covered in our previous publications particularly in Ref. 2 and are not repeated here. Sections A and E describe important new developments in our equipment and methods.

A. The Reaction Cell

Helium-filled reaction cells of small dimensions and high speed of recoil ion transport have been described in our previous papers.[2,3] The identical equipment was used in most of the work described here but in the later stages we devised and introduced a modified reaction cell which incorporates a few improvements. Figure 3 is a schematic diagram of the revised chamber. One important practical feature is that the target backing is no longer part of the entrance window so that it does not have to make a vacuum seal. The whole cell can be disassembled quickly and easily for target changes without the necessity to install carefully a new entrance window. Parts A and B in the cell can easily be replaced by similar but shorter pieces in case it is necessary to increase the He gas stopping path from the 1 cm length shown in the sketch.

The reaction cell is mounted in a fixed position inside a vacuum chamber connected to an external beam pipe of the HILAC. Chilled helium gas at a pressure of 2.2 atmospheres flows into the reaction cell interior via the input tube shown and escapes from the cell through a 0.4 mm inner diameter metal capillary. This capillary passes through a 1 mm hole in a gold surface barrier detector and terminates in a second vacuum chamber constantly evacuated to $\sim$ 200 μm Hg pressure by a high speed pump. The helium is pumped away but the recoil nuclei carried by the helium collect on a stationary metal collector positioned in front of the detector. This arrangement was suitable for study of activities with millisecond half lives. When the half life was longer than 1 second it was desirable to use a modified collection and counting technique (not illustrated in Fig. 3). The gas jet from the capillary tip impinged on the rim of a collector plate which could be held in one of two positions by a solenoid;[3] activity collected on the wheel rim for a pre-selected period of time was moved to a position in front of the detector.

The movement of the wheel lasted 0.1 sec during which period data recording was blanked out. Afterwards data could be recorded from the decaying sample and separately stored during 1 to 16 equally spaced decay periods. At the end of this time the wheel was moved back to its original collector position where it could collect a fresh sample; at the same time a second sample in a second spot (collected during the measurement time of the first sample) was ready for analysis.

B. Targets

The targets were in most cases made by vacuum evaporation of the metals onto a backing of 1.7 mg/cm^2 Ni. A few of the lead targets were electroplated. Separated lead and thallium isotopes were obtained from Oak Ridge National Laboratory and had the following isotopic compositions: ^{208}Pb 99.3%, ^{207}Pb 0.5%, and ^{206}Pb 0.2%; ^{208}Pb 1.4%, ^{207}Pb 1.3%, and ^{206}Pb 97.2%; ^{205}Tl 99.0% and ^{203}Tl 1.0%. The most usual thickness of the target material was 2-3 mg/cm^2 which is approximately equal to the range of the recoil atoms in the target.

C. Beam Energy Adjustment

The maximum available projectile energy was 10.3 MeV per nucleon for standard operation conditions at the HILAC. Lower beam energies were obtained by inserting stacks of 1.72 mg/cm^2 aluminum foils in front of the entry window of the reaction cell (see Fig. 3). The resulting beam energy, degraded by absorber foils, entrance window, target backing and the target material itself, was calculated by the use of Northcliffe's range-energy relationships.[5,6]

D. Alpha Standards

The primary calibration standards for our alpha spectra were taken from the actinium and thorium series,[7] in particular ^{211}Bi 6.622, ^{219}Rn 6.818 MeV, ^{215}Po 7.384 MeV, ^{212}Bi 6.051 MeV, and ^{212}Po 8.785 MeV. The calibration spectra were measured simultaneously with the reaction spectra in order to eliminate any possibility of slight gain shifts from beam-on and beam-off effects. Some known peaks in the reaction spectra were used as secondary alpha standards, particularly the following: ^{214}Ra 7.136 MeV, ^{215}Ra 8.698 MeV, ^{213}Fr 6.773 MeV, ^{214}Fr 8.426 MeV, and ^{214}Fr 8.549 MeV.

E. Time to Amplitude Converter Techniques for Measurement of Microsecond Daughter Activities

In each of the protactinium decay chains there occurs a daughter product with a half life in the microsecond range. We were able to measure these short half lives, to establish the relationship of the microsecond daughter to a specific parent, and to measure some details of the alpha group intensities for parent and daughter by development and use of the following two techniques. The first was discussed in our previous paper but we discuss here it as well as the second because both methods were of crucial importance for the results obtained in this study.

Both methods depend upon the fact that the alpha pulses coming from a detector which intercepts an appreciable percentage of the alpha particles emitted from a sample of genetically-related activities are not randomly distributed in time but include an appreciable number of pulse pairs separated by times, characteristic of the halflives involved in the chain. The time distribution of such pulse pairs, which is a measure of the half life involved, can be obtained by the use of a time-to-amplitude converter (TAC) operated in the microsecond time range.

The observed delayed-coincidence counting rate is proportional to the square of the effective solid angle of the detector. To increase that, the alpha activity was collected directly on the gold surface of a standard surface-barrier semiconductor detector.

TAC Method I. Our first TAC method, diagrammed in Fig. 4, was designed for use in those cases where the parent and daughter pulses, with pulse shaping settings available in our amplifier, were distinct pulses whose amplitudes could be measured separately. The TAC itself functioned in the normal way but one unconventional feature was that both start and stop signals came from the same detector. To prevent an individual pulse from serving simultaneously as start and stop, a delay was inserted on the start side. No pulse height selector was set on the start pulse. Any pulse received by the start input when the TAC was not busy could fire the TAC for its preset cycle time of 1 to 30 μsec and any second pulse reaching the stop input during this run-down time could cause the development of a linear pulse on the time output of the TAC. This time pulse was passed to a computer interface unit. The linear signals associated with the start and stop pulses were also passed to the computer, but in order to insure time overlap of all three pulses it was necessary to include the pulse stretching and gating circuitry shown in Fig. 4. To permit examination of halflives as short as 1 μsec time constants of 0.2 μsec were used in the pulse shaping network of the main amplifier.

A computer program, MULTID, was used to control the acceptance and processing of the pulses by a PDP-7 computer. Whenever signals appeared simultaneously on the three inputs the pulse amplitudes were coded and stored as an event record on magnetic tape. The distributions over the three parameters were shown on-line during data recording. After the experiment, the events on the

magnetic tape record were analyzed with the program MULTIS by setting selection criteria (windows) on any two of the three parameters and examining the corresponding distribution of the third. For example, windows could be set on specific alpha peaks in the start (parent) and stop (daughter) spectra and the corresponding time spectrum examined to determine the half-life of a specific nuclide. In a second sort windows could be set to permit examination of the entire start spectrum corresponding to specific regions of the stop and time spectrum.

TAC Method II. The above method is successful when the daughter half-life is long compared to the width of the individual parent or daughter pulses. Attempts to reduce pulse widths below 0.2 μsec resulted in serious deterioration of the quality of the signal. In the case of a submicrosecond half-life an overlap or pile-up of the parent-daughter pulses occurs and there is a loss of distinct pulses containing the energy information. In this case it is possible to emphasize the pile-up deliberately by use of quite long time constants for pulse shaping (5 μsec for example) and to make an accurate measurement of the amplitude distribution of the sum pulses. A scheme for performing the experiment in this manner is shown in Fig. 5. The electronic scheme was simpler in this case because no pulse stretcher was needed; the acceptance time for the multidimensional computer interface was 3 μsec and the TAC range was set to 3 μsec or less.

After the experiment the information stored on magnetic tape was analyzed as described above under method I, except here there was only one energy spectrum and consequently no information on which α-pulse came first. Sorting of the data according to specific peaks in the sum spectrum was still of great use because it revealed time parameter information characteristic of specific mother-daughter combinations.

We owe thanks to Drs. R. D. MacFarlane and D. F. Torgerson[8,9] for the initial suggestion of the application of a time-to-amplitude converter to problems of this type.

III. RESULTS

A. Protactinium-225 Series

The first investigation of ^{225}Pa was made in 1951 by Keys[10] who bombarded thorium with high energy deuterons and measured the alpha particle energies of the ^{225}Pa decay series by a nuclear emulsion technique. He reported the decay sequence to be:

$^{225}Pa \xrightarrow{\alpha}$	$^{221}Ac \xrightarrow{\alpha}$	$^{217}Fr \xrightarrow{\alpha}$	$^{213}At \xrightarrow{\alpha}$	^{209}Bi
	7.6 MeV	8.3 MeV	9.2 MeV	
∿ 2 sec	<< 1 sec	<< 1 sec	<< 1 sec	stable

Tove[11] later revised the ^{225}Pa half life to 0.8 ± 0.1 sec. More definite information on the entire series was provided in the 1969 work of Hahn, Roche, and Toth[12] who bombarded ^{233}U with protons and produced ^{229}Np by the (p,5n) reaction. These authors formulated the decay sequence as Keys did with the addition of a 4.0 min ^{229}Np precurser. Their alpha-particle energy data, determined by Si(Au) semiconductor detectors are summarized in Table II together with the results obtained in the present study.

We were able to use several combinations of targets and heavy-ion projectiles to make individual members of the decay chain. However, in the case of ^{229}Np the only possibility among those open to us was the $^{209}Bi(^{22}Ne, 2n)^{229}Np$ reaction and the cross section, even at the Coulomb barrier, proved to be too low

because of severe fission competition. We were able to make samples of ^{255}Pa with the $^{209}Bi(^{22}Ne, \alpha 2n)^{225}Pa$ reaction as shown by the spectra in Fig. 6, but with no improvement in intensity over the spectra published by Hahn et al.[12] The ^{221}Ac member was easily produced in the $^{208}Pb(^{19}F, \alpha 2n)^{221}Ac$, the $^{205}Tl(^{22}Ne, \alpha 2n)^{221}Ac$, and the $^{208}Pb(^{16}O, p2n)^{221}Ac$ reactions. Spectra from the first two of these reactions are presented in Figs. 8 and 10; those from the $^{208}Pb + ^{16}O$ combination are given in Fig. 6 of our report on the thorium isotope decay chains.[2] Some other spectra shown in that report also show traces of the ^{225}Pa series produced by "proton-out" reactions in the interactions of $^{209}Bi + ^{19}F$, $^{208}Pb + ^{22}Ne$, and $^{208}Pb + ^{20}Ne$, but these reactions provide only minor supporting evidence for the detailed conclusions discussed below.

1. Protactinium-225

Hahn et al.[12] report a single group for ^{225}Pa at 7.25 MeV. We observe this group at 7.245 ± 0.010 MeV in the $^{209}Bi + ^{22}Ne$ spectrum in Fig. 6. There may exist a second group at 7.195 ± 0.010 MeV with about 1/5 the intensity of the 7.245 MeV peak. The excitation functions determined for these peaks are shown in Fig. 7. They differ only slightly from those of ^{217}Fr and ^{213}At, as should be the case if the assignments are correct. We remeasured the half life of ^{225}Pa by observing the decay of the 8.31 MeV group of ^{217}Fr and the 9.08 MeV group of ^{213}At in samples prepared by the $^{209}Bi(^{22}Ne, \alpha 2n)^{225}Pa$ reaction. The ^{225}Pa was collected for 16 seconds and its decay followed throughout 16 one-second time periods. A half life value of 1.8 ± 0.3 seconds was obtained. The alpha particle group at 7.245 MeV may be the ground state transition as it fits smoothly in the protactinium curve in Fig. 2.

2. Actinium-221

Hahn et al.[12] assign groups of 7.63 and 7.42 MeV energy to ^{221}Ac. We assign groups at 7.645, 7.440, 7.375, and 7.170 MeV to ^{221}Ac with the intensity and error values listed in Table II. These assignments are based on excitation functions and on the observation of a common half life of roughly 50 msec for each of these peaks. Detailed consideration of data from many experiments and evaluation of contributions from alpha groups of similar energy from other nuclides was necessary to extract the intensity values.

The 7.645 MeV group is mixed with the 7.68 MeV group of the partial transfer reaction product ^{212}At and this leads to a broadening of the apparent excitation functions (Figs. 9 and 11) and to complexity in the half life curves for this group. Nonetheless, the half life measurements at 105 MeV beam energy in the ^{208}Pb + ^{19}F reaction and at 100-110 MeV beam energy in the ^{205}Tl + ^{22}Ne reaction clearly show the presence of the 50 msec component. The 7.440 MeV group is similarly masked by the 7.448 MeV group of ^{211}Po produced in the partial transfer reaction and the composite peak has a broad excitation function as shown in Figs. 9 and 11 as well as in Fig. 7 of Ref. 1. Half-life measurements on this peak reveal the presences of a 50 msec component and permit an estimate of the ^{221}Ac group intensity.

In addition to these two groups there is evidence for two more in the ^{221}Ac spectrum at 7.375 ± 0.010 MeV and 7.170 ± 0.010 MeV with intensities of 10 ± 5% and ∿ 2%, respectively. These groups appear in Figs. 8 and 10 and in other spectra. The excitation functions shown in Figs. 9 and 11 resemble those of the other members of the ^{225}Pa chain. Half-life measurements on these peaks were of low statistical accuracy but gave values of about 50 msec. It is worthy of

note that this half life is far too short to permit confusion of the 7.17 MeV group with a group of like energy in ^{224}Th.

Strong proof of the identity and relative intensity of the 3 most intense peaks of ^{221}Ac came from measurements made by the special TAC technique. These measurements are described in Sec. III A5.

The best value of the half life of ^{221}Ac came from measurements of the decay of the 8.315 MeV peak of ^{217}Fr which is in equilibrium with ^{221}Ac in the products of the ^{208}Pb + ^{19}F and ^{205}Tl + ^{22}Ne reactions. The value obtained was $t_{1/2}$ = 52 ± 2 msec.

3. Francium-217

This nuclide has a single alpha group at 8.315 ± 0.008 MeV which fits smoothly on the alpha-systematics curve in Fig. 2. The excitation curves in Figs. 9 and 11 and in Figs. 3, 5, and 14 of Ref. 1 have yield maxima such that there is no question of the assignment. In several reactions in which we might have expected some direct production of ^{217}Fr such as in the ^{208}Pb + ^{14}N, ^{208}Pb + ^{12}C, and ^{208}Pb + ^{11}B combinations we saw none, which is consistent with the 22 ± 5 μsec half life, discussed in subsection 5 below.

4. Astatine-213

We assign a peak at 9.080 ± 0.012 to ^{213}At. This peak appears in all our spectra in which ^{225}Pa or ^{221}Ac are present. The yield curves in Figs. 9 and 11 as well as in Fig. 7 of Ref. 1 support the assignment as does also the value of 50 msec measured for the apparent half life of the group, the measured half-life being that of the ^{221}Ac parent. The true half life of ^{213}At was obtained by the TAC techniques as discussed in the following section; the value is 0.11 ± 0.02 μsec.

5. Additional Measurements by TAC Technique

The short half lives of ^{217}Fr and ^{213}At made them suitable candidates for study by the special techniques employing a time-to-amplitude converter (TAC) which are discussed in Sec. IIE. We applied these methods to the products of the $^{208}Pb + ^{19}F$ reaction at a bombarding energy of 115 MeV.

The results of a TAC experiment done by Method I are shown in the several spectra of Fig. 12. In this experiment the pulse shaping constants for the main amplifier were set at 0.2 μsec and a delay of 2 μsec was used on the start input to the TAC. The unsorted start spectrum shows the energy distribution of those pulses which are followed by a second alpha pulse within the 25 μsec inspection time of the TAC, while the unsorted stop spectrum shows the corresponding energy distribution of the alpha pulses functioning as stop signals. The accompanying time spectrum is not shown. The most prominent peaks in the start spectrum are those of ^{221}Ac and in the stop spectrum are those of ^{217}Fr and ^{213}At. No ^{217}Fr appears in the start spectrum because the 0.11 μsec half life of ^{213}At is short compared to the 2 μsec delay time on the start signal input. On the other hand a ^{213}At pulse could serve as a stop signal for a TAC cycle started by its grandparent ^{221}Ac if the intermediate ^{217}Fr alpha particle did not enter the detector.

There are other peaks in the unsorted stop and start spectra because of the presence of other microsecond activities in the sample. These contaminants were removed from the spectra by suitable off-line sorts with the MULTIS program after setting windows on peaks in the start and stop spectra. (See labelled windows in Fig. 12.) A data sort with the window A (corresponding to the 7.65 and 7.44 MeV peaks of ^{221}Ac) set on the start spectrum produced the stop spectrum shown in Fig. 12d with peaks for ^{217}Fr(8.31 MeV) and ^{213}At(9.08 MeV) in equal

intensity. A sort with windows B and C set on the ^{217}Fr and ^{213}At peaks in the stop spectrum and no time restriction produced the start spectrum of ^{221}Ac peaks shown in Fig. 12c. This spectrum verifies our previous assignment of 3 peaks at 7.65, 7.44, and 7.38 MeV to ^{221}Ac. The relative intensities of these peaks are 70, 20, and 10. The intensity was too low to reveal a peak at 7.17 MeV in two percent. The half life of ^{217}Fr came from a data sort with windows set on the ^{217}Fr peak in the stop spectrum and on the ^{221}Ac peaks in the start spectrum. The decay curve yielded a value of 22 ± 5 μsec as shown in Fig. 13.

The half life of ^{213}At was measured by a different experiment done by the TAC technique Method II discussed in Sec. IIE. In this experiment the delay time on the start input of the TAC was reduced to 80 nsec and the differential and integrating time constants for the main amplifier were increased to 5 μsec to maximize the effect of pile up of the ^{217}Fr and ^{213}At pulses. The amplifier gain was reduced a factor of 2 to permit inspection of the sum pulses of 17.4 MeV energy. The cycle time of the TAC was set at 3 μsec. Samples were collected directly on the surface of the detector. In the unsorted alpha sum spectrum obtained in this experiment (see Fig. 14) the 17.4 MeV peak was prominent but there was also present a complex sum from the pile up of ^{216}Fr + ^{220}Ac (see discussion in Sec. B below). An off-line sort with window set around the 17.4 MeV peak (see window B in Fig. 14) produced a time spectrum characteristic only of the ^{213}At decay. This spectrum, which is shown as Fig. 15, determines a rough half-life value of 0.08 μsec. A more accurate value of 0.11 ± 0.02 μsec was obtained from a nearly identical experiment in which a more suitable TAC cycle time of 1 μsec was used. See Fig. 16.

These TAC experiments provide very strong evidence for our deductions on the genetic relationships within the ^{225}Pa decay series.

B. The Protactinium-224 Series

No published information is available on the properties of ^{224}Pa but our data establish that the ^{224}Pa series has the following form:

$$^{224}Pa \xrightarrow{\alpha} \quad ^{220}Ac \xrightarrow{\alpha} \quad ^{216}Fr \xrightarrow{\alpha} \quad ^{212}At \xrightarrow{\alpha} \quad ^{208}Bi$$

0.95 sec 26.1 msec 0.70 μsec 305 msec 3.7×10^{5} y

Our detailed conclusion on ^{224}Pa, ^{220}Ac, and ^{216}Fr are summarized in Table II.

The most useful target-projectile combination was ^{205}Tl + ^{22}Ne. Spectra and yield curves are shown in Figs. 10 and 11. The combination ^{208}Pb + ^{19}F also produces the ^{224}Pa series but side reactions leading to the direct production of several interfering activities--notably ^{211}Po, ^{211m}Po, ^{212}At, and ^{212m}At--are prominent when this target-projectile combination is used. See Figs. 8 and 9. It was not difficult to establish the main features of the decay chain but it was hard to identify and determine the correct intensities for the alpha groups in the complex spectra for ^{224}Pa and ^{220}Ac. One complicating factor was that the ^{225}Pa chain was present to some extent in most of the samples and the complex alpha groups of ^{221}Ac appeared in the energy region of interest. However, the bombardment of ^{208}Pb with ^{15}N at an energy just above the Coulomb barrier resulted in a remarkably clean spectrum of ^{220}Ac. Additional supporting evidence came from some of the other reactions listed in Table I. The individual members of the series are discussed in the following sections.

1. Comment on ^{228}Np

The nuclide ^{224}Pa could have a parent ^{228}Np produced by the (^{22}Ne, 3n) reaction in the case of ^{209}Bi bombarded by ^{22}Ne, but we found no evidence for

^{228}Np alpha groups in the 7.3 - 7.5 MeV energy range where they might be expected according to the neptunium curve in Fig. 2. This absence is the result of removal of the neptunium nuclei by nuclear fission.

2. Protactinium-224

The most definite evidence for ^{224}Pa came from the reactions ^{205}Tl(^{22}Ne, 3n)^{224}Pa and ^{208}Pb(^{19}F, 3n)^{224}Pa where the maximum yield occurs close to the Coulomb barrier. A peak of 7.49 MeV energy can be seen in the curves for the lowest bombarding energies in Figs. 8 and 10. This peak has a narrow excitation function with a maximum close to the barrier as can be seen in Figs. 9 and 11. We assign this peak to ^{224}Pa. It is unlikely that it is the only alpha group emitted by ^{224}Pa because generally odd-odd nuclei have quite complex alpha-decay patterns. It is possible that small peaks at 7.88 ± 0.02 MeV and 7.96 ± 0.02 MeV belong to ^{224}Pa and that other groups are hidden in our spectra. We are thus left with uncertainty as to the proper value to use for ^{224}Pa in Fig. 2. It seems unlikely that the 7.49 MeV group can be the ground-state transition.

The excitation function for ^{224}Pa does not resemble those of ^{220}Ac and ^{216}Fr for the reason that ^{220}Ac is formed only partially from the decay of ^{224}Pa; it is produced in greater yield from "alpha-out" reactions.

Strong evidence for ^{224}Pa came from a half life measurement made on the products of the ^{208}Pb + ^{19}F reaction at 106 MeV beam energy. In this measurement the sample was collected during a bombardment period of 3 seconds. Then the beam was interrupted and alpha spectra were recorded separately for the time periods of 0.25 seconds each. It was observed that the 9.01 MeV group of ^{216}Fr decayed with a half life of 0.95 ± 0.15 sec. This could be true only if a 0.95 sec ^{224}Pa were present to support the series since ^{220}Ac and ^{216}Fr have much shorter half lives.

3. Actinium-220 and Francium-216

Actinium-220 decays by emission of the seven alpha groups listed in Table III. In most of our experimental spectra it was not possible to make a clear resolution of several of these peaks because of interference from alpha groups of ^{221}Ac, ^{223}Pa and the isomers of ^{214}Fr and ^{212}At. However, in the $^{208}Pb(^{15}N, 3n)$ reaction, ^{220}Ac is prepared in a nearly pure state (Fig. 17). Only in the 7.68 MeV group is there some interference (from ^{212}At) but a half life measurement showed that 50% of the group was ^{220}Ac.

The half life of ^{220}Ac was measured in an experiment in which a sample was collected during a 104 msec period and then, with the beam off, the alpha spectrum was recorded for 16 time periods of 20 msec each. The decay of individual peaks of ^{220}Ac and of the 9.005 MeV peak of ^{216}Fr was plotted separately. The most accurate value of the half life (26.1 ± 0.5 msec) came from the decay of the ^{216}Fr peak as shown in Fig. 18.

Francium-216 appears to emit a single alpha group of 9.005 ± 0.010 MeV which value fits smoothly on the francium curve in Fig. 2.

The TAC method I was applied to ^{220}Ac samples prepared by the $^{208}Pb + ^{15}N$ reaction as shown in Fig. 19 which represents a data sort with the condition imposed that all stop pulses have an amplitude corresponding to the 9.005 MeV ^{216}Fr group. Such a sort eliminates ^{212}At and any other possible contaminants from the spectrum and confirms the presence of major ^{220}Ac groups at 7.61 and 7.68 MeV. The residual peak of ^{216}Fr is attributed to accidental occurrence of unrelated pulses within the 3 μsec TAC range. The time parameter information associated with the data sort displayed in Fig. 19 is plotted in Fig. 20 to show the 0.70 ± 0.02 μsec half life of ^{216}Fr.

The sum-spectrum displayed previously in Fig. 14 has a broad peak which can be assigned to ^{220}Ac + ^{216}Fr. This broadness can be attributed to the many α-groups of ^{220}Ac which individually sum with the 9.005 MeV group of ^{216}Fr. A sort of these data with window A set on the ^{220}Ac + ^{216}Fr peak produced the ^{216}Fr half life curve shown in Fig. 15.

C. Protactinium-223 Series

There exist no published data on ^{223}Pa and on its decay products ^{219}Ac and ^{215}Fr. In Figs 8, 10 and 21 there are several alpha peaks which we attribute to these nuclides. We conclude that ^{223}Pa is formed in small yield by the reactions $^{208}Pb(^{19}F, 4n)^{223}Pa$, $^{205}Tl(^{22}Ne, 4n)^{223}Pa$, and $^{209}Bi(^{20}Ne, \alpha 2n)^{223}Pa$, and that the decay goes as follows:

$$\begin{array}{ccccccc} ^{223}Pa & \xrightarrow{\alpha} & ^{219}Ac & \xrightarrow{\alpha} & ^{215}Fr & \xrightarrow{\alpha} & ^{211}At \\ 6\ \text{msec} & & 7\ \mu\text{sec} & & < 0.5\ \mu\text{sec} & & 7.2\ \text{hr} \end{array}$$

The alpha-particle energies are summarized in Table II.

These conclusions are based on the following arguments. The alpha groups appear together in all spectra. The energies have values in agreement with the trends in Fig. 2. The assignment of the 9.365 MeV group to ^{215}Fr seems particularly secure owing to the very restricted number of possible assignments of alpha groups above 9.3 MeV energy. The excitation function of the 9.365 MeV group has a maximum at 105 MeV for the 3 reaction systems studied (see ^{215}Fr curves in Fig. 9, 11 and 22), which is a reasonable energy for maximum production of ^{223}Pa via the reactions written above. The excitation function curves for the 8.66 MeV ^{219}Ac peak have nearly the same form (Fig. 11) except for some distortion caused

by some interferring 8.675 MeV ^{215}Rn present as the result of side reactions. In the case of the ^{223}Pa groups at 8.00 and 8.19 MeV there is serious interference from ^{220}Ac groups of similar energy so that the excitation function curves are composite. In agreement with this it was found that the decay curves for these peaks included half-life components of 6 and 22 msec. With the aid of this time information we were able to decompose the excitation function curves for the two alpha groups into ^{223}Pa and ^{220}Ac fractions and to determine values of 45 ± 5% and 55 ± 5% for the 8.19 and 8.00 MeV peaks, respectively, of ^{223}Pa. The same abundance values were obtained from the analysis of the ^{208}Pb + ^{19}F and ^{205}Tl + ^{22}Ne experiments even though the relative amounts of ^{223}Pa and ^{220}Ac were quite different with these two target-projectile combinations.

The final proof of the genetic relationship of these alpha groups came from measurements made by the TAC techniques as discussed below.

1. Half life of ^{223}Pa

To measure the half life of ^{223}Pa a target of ^{205}Tl was bombarded with 105 MeV ^{22}Ne ions and data were collected on the alpha-emitting products by a controlled sequence in which the beam was on for 200 msec then blanked off for an 80 msec period during which the alpha spectrum was recorded separately for 8 time periods of 10 msec each. This sequence was repeated for a 2 hour period. The intensity of the 8.18 MeV ^{223}Pa peak, the 8.66 MeV ^{219}Ac peak, and the 9.365 MeV ^{215}Fr peak was plotted versus the time elapsed from the time of beam interruption. Similar experiments were performed for ^{208}Pb bombarded with 100 MeV ^{19}F ions. From the combined results a value of 6.5 ± 1.0 msec was determined for the ^{223}Pa half life.

2. Measurements by the TAC techniques

An application of the TAC techniques to some products of the ^{208}Pb + 115 MeV ^{19}F reaction is discussed in Sec. III A5. (See Fig. 12). The principal purpose of those measurements was to determine the properties of the $^{221}Ac \longrightarrow {}^{217}Fr \longrightarrow {}^{213}At$ sequence. It can be noted however that the 8.00 and 8.19 MeV ^{223}Pa peaks are present in the unsorted start spectrum (Fig. 12a) and that the 8.66 MeV ^{219}At and 9.36 MeV ^{215}Fr peaks are present in the unsorted stop spectrum. This is so because there is an appreciable yield of the ^{223}Pa series at this bombardment energy and because the ^{219}At and ^{215}Fr pulses follow the ^{223}Pa pulses within the 25 μsec cycle time used for the TAC. Little or no ^{219}At appears in the start spectrum because the ^{215}Fr is short lived compared to the pulse shaping times of the parent and daughter pulses. Alpha summing occurs in this case and the event is lost to the data record. (That such summing indeed occurs is shown by the ^{219}Ac + ^{215}Fr sum peak in Fig. 14). However, if a ^{223}Pa alpha pulse starts the TAC sequence and the ^{219}Ac daughter alpha does not enter the detector, the alpha particle from the granddaughter ^{215}Fr may still enter the detector and generate a stop pulse. In this case the ^{215}Fr alpha group appears in the stop spectrum. These observations permit us to estimate a conservative upper limit of 0.5 μsec for the ^{215}Fr half life.

Data sorting by the MULTIS program provided additional data. When we imposed the requirement that the stop pulse have the 8.66 MeV energy of ^{219}Ac the sorted start spectrum contained mainly the 8.00 and 8.19 MeV groups of ^{223}Pa. A third peak appeared in this sorted start spectrum at 7.68 MeV. This is explained by the fact that the 8.66 MeV peak in the stop spectrum is not pure ^{219}Ac but a mixture of this with ^{215}Rn which decays with a 2.5 μsec half life after formation from its ^{219}Ra parent. This extraneous ^{219}Ra peak was removed from the start

spectrum by another data sort in which the requirement was imposed that the stop pulse have the energy of the ^{215}Fr peak. (In Fig. 12 the ^{215}Fr peak energy is somewhat low owing to amplifier saturation.) In this case only the 2 peaks of ^{223}Pa appeared in the start spectrum, in the relative intensities reported above. The time plots corresponding to these data sorts revealed a one-component half life of 7 ± 2 μsec for the half life of ^{219}At.

D. Protactinium-222 Series

During the course of this work it was established that the unknown nuclide ^{222}Pa undergoes decay in the following manner:

$$^{222}Pa \xrightarrow[5.5\ \text{msec}]{8.16\text{-}8.54\ \text{MeV}\ \alpha} {}^{218}Ac \xrightarrow[0.27\ \mu\text{sec}]{9.205\ \text{MeV}\ \alpha} {}^{214}Fr$$

The clearest evidence came from the $^{209}Bi(^{16}O, 3n)^{222}Pa$ and $^{206}Pb(^{19}F, 3n)^{222}Pa$ reactions (see Fig. 23 and 24) but several other target-projectile combinations gave useful information as indicated in Table I. In these figures we note a prominent peak at 9.21 MeV. The possible assignments of an alpha energy of this magnitude are extremely limited (see Fig. 2); the favored assignment is to ^{218}Ac. The maximum in the excitation function for this peak in Fig. 25 falls at 89 MeV which is a reasonable value for the $(^{16}O, 3n)$ reaction.

^{218}Ac has a 0.27 μsec half life (see below) so that it appears in these spectra only by its continued replenishment by the decay of ^{222}Pa. Peaks at 8.18 MeV (complex), 8.33, and 8.54 MeV are assigned to ^{222}Pa. The 8.18 MeV group in Fig. 24 is too broad to be single and in Fig. 23 we show a possible decomposition into three groups of 8.16, 8.18 and 8.21 MeV. Hence, we list 5 groups for ^{222}Pa in Table II but it is quite likely that other groups of lower intensity remain to be found.

The composite 8.18 MeV peak has the same form for its yield curve in Fig. 25 as does ^{218}Ac. The 8.33 MeV group is badly mixed with the 8.36 MeV group of ^{214}Fr. The 8.54 MeV peak is mostly ^{222}Pa but is mixed with some ^{214m}Fr. It is known that ^{214m}Fr has peaks at 8.48 and 8.55 MeV of nearly equal intensities so a correction can be made for the ^{214m}Fr contribution to the 8.54 MeV peak.

A half-life measurement was made on samples prepared by the ^{209}Bi + ^{16}O reaction by a data recording sequence in which the 20 msec period between beam pulses was divided into 12 time periods of 1.7 msec and the alpha spectrum was recorded separately for these time periods. The intensity of each alpha group of interest was plotted against time to determine half life curves for individual peaks. The 8.18 MeV ^{222}Pa peak and the 9.21 MeV ^{218}Ac peak provided the best data leading to a value of 5.7 ± 0.5 msec for the ^{222}Pa half life.

The half life of ^{218}Ac was measured in an experiment done by the TAC method I described in the Sec. IIE. In this experiment the products of the ^{209}Bi + ^{16}O reaction were studied at a beam energy of 95 MeV. The 9.21 MeV ^{218}Ac peak appeared in the stop spectrum. The data were sorted with the MULTIS program with a window set on the ^{218}Ac peak in the stop spectrum and another across the region of the ^{222}Pa groups in the start spectrum in order to derive a time distribution characteristic of ^{218}Ac. This resulted in a one-component decay curve corresponding to a half life of 0.27 ± 0.04 μsec. A second sort isolated the ^{222}Pa groups associated with the ^{218}Ac daughter activity. The intensity of the ^{222}Pa peaks in this sorted start spectrum was quite low (about 100 counts total) but these were grouped at the expected energies of 8.18, 8.33, and 8.55 MeV, which verifies the assignment to ^{222}Pa.

IV. DISCUSSION

A. Possible Presence of Long-Range Alpha Particles

The observation in this and in the previous study[1] of several nuclides emitting alpha particles of more than 9 MeV with extremely-short halflives makes it necessary to consider the possible occurrence of alpha emission from excited states in competition with γ-emission. From known relationships between alpha-decay energy and halflife we can expect alpha decay halflives for $E_\alpha > 9.0$ MeV to fall in the range 10^{-8} to 10^{-6} sec for isotopes of the elements polonium through radium. Gamma ray halflives for single particle transitions are of this order or longer for gamma transitions of higher multipolarity than E1 or M1 provided the γ-transition energy is less than 200 keV. Thus, the distinct possibility exists that some of the alpha groups in our spectra correspond to alpha transitions from excited states. We believe that all the alpha peaks given definite assignments in this report are correctly regarded as transitions from a ground state but some unidentified low-intensity peaks of > 9.0 MeV are possible candidates for attribution to alpha transitions from excited levels. Further work is required to identify and assign these alpha groups.

B. Systematic Trends in Alpha Data

The systematic trends in the experimental alpha-particle energies for the ground-state transitions of all known alpha emitters of odd Z near the 126 neutron shell are displayed in Fig. 2. The new data on protactinium, actinium, and francium isotopes obtained in the present work help to define the trends on the right side of the spike at 128 neutrons and make it possible to estimate decay energies for lighter nuclei which have not yet been measured. A similar plot of the data for even Z elements is given in Fig. 17 of our previous paper.[1]

In those few cases where there is doubt that the measured experimental values represent decay to the ground state the points are drawn with special arrows to call attention to this uncertainty. We noticed that most of these doubtful points occurred for nuclei with neutron number 133 or 135 and decided to replot the data in the manner displayed in Fig. 26. In this figure it can be seen that the experimental points lie systematically low for the N = 133 isotones of Fr, Ra, Ac, Th and Pa. The squares indicate the values which seem to us more correct for the trends in this figure and in the previously cited figures. There are no experimental data against this interpretation except in the case of ^{221}Ra where the alpha-gamma coincidence spectra of Ruiz[14] seem to establish that the 6.754 MeV alpha particle reaches the daughter ground state. This work is not completely definitive however and would, for example, not have detected a delayed and perhaps highly-converted transition of the daughter nucleus to its true ground state.

The question arises whether some individual particle level of high spin occurs at or near neutron number 133 to cause a sudden change in the

alpha-decay pattern. Inspection of the shell model level diagram for spherical nuclei indicates no likelihood of this. On the other hand, if we admit the possibility of significant nuclear distortion for such nuclei as ^{220}Fr, ^{221}Ra, ^{222}Ac, ^{223}Th and ^{224}Pa then the Nilsson model level scheme should be applicable. If we consult a recent paper of S. G. Nilsson and co-authors[15] and particularly Fig. 2f of that reference we note that for nuclei near mass 225 with an ε parameter of ~ 0.2 and a slight ε_4 distortion of -0.04 the [606]13/2-level is favored for the 131st and 132nd neutron and that the neighboring orbitals have spins of 3/2, 5/2 and 1/2. This indicates that these irregularities in alpha-particle energies may be connected with the onset of stable ground-state deformation in this group of nuclei and with the occurrence of a 13/2 level near 133 neutrons. The possibility of isomerism is also indicated. These considerations indicate that the nuclei in this region are worth further study.

It is also of interest to compare the experimental alpha-particle energies and the estimated alpha-particle energies (squares in Figs. 2 and 26) with the predictions of various mass formulae and semiempirical estimation methods.[16-19] We have done this in Table III after converting the alpha-particle energy to a Q value corrected for the recoil energy and for the screening effect of the atomic electrons. In order to judge the success of these predictions for this particular group of nuclei we have made plots (not shown) of the data sets from Table III. From these we conclude that the extrapolations by Viola and Seaborg[18] are in best agreement with our experimental data with a mean deviation of 90 keV. Among the mass formulae the predictions by Garvey et al.[17] and Zeldes et al.[19] reproduce well the trend of the experimental

points and differ in the absolute values by mean deviations of only 150 keV and 200 keV, respectively. The values of Myers and Swiatecki show a considerably different trend and deviate from the experimental points by more than 1 MeV in the worst cases.

It may also be of some interest to apply a widely-used semiempirical formula relating half-life and alpha decay energy to the new half-life information an odd-odd and odd-even nuclei reported in this paper as well as to new life time data in even-odd nuclei reported in the previous paper. We use the relationship

$$\log_{10} t_{1/2} = A_Z Q_{eff}^{-1/2} + B_Z + \log_{10} F$$

where $t_{1/2}$ is the partial half life in seconds, Q_{eff} is the alpha decay energy in MeV, A_Z and B_Z are empirical constants, and F is the empirical hindrance factor. Table IV gives values of $\log_{10}F$ for 15 alpha emitters based on A_Z and B_Z constants interpolated from values given by Viola and Seaborg.[18]

V. ACKNOWLEDGMENTS

One of us (KV) expresses his appreciation to the National Research Council for Sciences in Finland for financial support during part of the work recorded here. One of us (JB) expresses his thanks for a fellowship from the North Atlantic Treaty Organization. We owe thanks to C. A. Corum for mechanical design work, to A. A. Wydler and R. G. Leres for advice on electronic problems, and to Dr. L. Robinson for his many contributions to the PDP-7 computer system including the programming for the MULTID and MULTIS codes mentioned in the text. Finally we thank the crew of the HILAC for its indispensable assistance.

FOOTNOTES AND REFERENCES

* Work performed under the auspices of the U. S. Atomic Energy Commission.

† Permanent address: Niels Bohr Institute, Copenhagen, Denmark.

†† Present address: Department of Physics, University of Helsinki, Helsinki, Finland.

1. K. Valli, E. K. Hyde, and J. Borggreen, University of California Lawrence Radiation Laboratory Report UCRL-18992, October 1969; accepted for publication in the Physical Review (1970).
2. K. Valli and E. K. Hyde, Phys. Rev. 176, 1377 (1968).
3. K. Valli, W. J. Treytl, and E. K. Hyde, Phys. Rev. 167, 1094 (1968).
4. R. D. MacFarlane, R. A. Gough, N. S. Oakey, and D. F. Torgerson, Nucl. Instr. Methods 73, 285 (1969).
5. L. C. Northcliffe, Phys. Rev. 120, 1744 (1960).
6. L. C. Northcliffe, Ann. Rev. Nucl. Sci. 13, 67 (1963).
7. A. Rytz, Phys. Acta. 34, 240 (1961).
8. D. F. Torgerson and R. D. MacFarlane, private communication, 1969.
9. D. F. Torgerson, Ph.D. Thesis, McMaster University, (1969).
10. J. D. Keys, Ph.D. Thesis, McGill University (1951).
11. P. A. Tove, Arkiv Fysik 13, 549 (1958).
12. R. L. Hahn, M. F. Roche, and K. S. Toth, Nucl. Phys. A113, 206 (1968).
13. D. F. Torgerson, R. A. Gough and R. D. MacFarlane, Phys. Rev. 174, 1494 (1968).
14. C. P. Ruiz, Ph.D. Thesis, University of California (1961), Lawrence Radiation Laboratory Report UCRL-9511.
15. S. G. Nilsson, C. F. Tsang, A. Sobiczewski, Z. Szymański, S. Wycech, G. Gustafson, I. L. Lamm, P. Möller and B. Nilsson, Nucl. Phys. A131, 1 (1969).

16. W. D. Myers and W. J. Swiatecki, Arkiv Fysik 36, 343 (1967).

17. G. T. Garvey, W. J. Gerace, R. L. Jaffe, I. Talmi, and I. Kelson, Rev. Mod. Phys. 41, 1 (1969).

18. V. E. Viola and G. T. Seaborg, J. Inorg. Nucl. Chem. 28, 697 (1966) and 28, 741 (1966).

19. N. Zeldes, A. Grill, and A. Simievec, Mat. Fys. Skr. Dan. Vid. Selsk. 3, (1967) No. 5.

Table I. General Summary of Target Projectile Combinations

Target, Projectile and Compound Nucleus	Level of Usefulness for Production and Study of members of Protactinium decay Chains		
	High	Moderate	Low
$^{209}Bi + ^{22}Ne \rightarrow ^{231}Np$		^{225}Pa, ^{224}Pa	^{223}Pa
$^{209}Bi + ^{20}Ne \rightarrow ^{229}Np$		^{224}Pa	^{223}Pa, ^{222}Pa
$^{208}Pb + ^{22}Ne \rightarrow ^{230}U$			^{225}Pa, ^{224}Pa
$^{208}Pb + ^{20}Ne \rightarrow ^{228}U$			^{225}Pa, ^{224}Pa
$^{209}Bi + ^{19}F \rightarrow ^{228}U$			^{225}Pa, ^{224}Pa
$^{208}Pb + ^{19}F \rightarrow ^{227}Pa$	^{224}Pa, ^{221}Ac, ^{220}Ac	^{223}Pa, ^{222}Pa	
$^{205}Tl + ^{22}Ne \rightarrow ^{227}Pa$	^{224}Pa, ^{221}Ac, ^{220}Ac	^{223}Pa, ^{222}Pa	
$^{205}Tl + ^{20}Ne \rightarrow ^{225}Pa$		^{222}Pa	^{220}Ac
$^{209}Bi + ^{16}O \rightarrow ^{225}Pa$		^{222}Pa, ^{220}Ac	
$^{206}Pb + ^{19}F \rightarrow ^{225}Pa$		^{222}Pa	
$^{208}Pb + ^{18}O \rightarrow ^{226}Th$	^{221}Ac, ^{220}Ac		
$^{208}Pb + ^{16}O \rightarrow ^{224}Th$	^{221}Ac, ^{220}Ac		
$^{208}Pb + ^{15}N \rightarrow ^{223}Ac$	^{220}Ac		
$^{208}Pb + ^{14}N \rightarrow ^{222}Ac$		^{220}Ac	

Table II. Summary of Results on Protactinium Decay Chains

Nuclide	Present Results: α-Particle energy (MeV)	Present Results: Intensity %	Present Results: $T_{1/2}$	Previous Reports: α-Particle energy (MeV)	Previous Reports: Intensity %	Previous Reports: $T_{1/2}$
^{229}Np chain						
^{229}Np				6.89[a]	100	4.0 min[a]
^{225}Pa	7.195 ± 0.010(?)	30 ± 10	1.8 ± 0.3sec			∿ 2 sec[b]
	7.245 ± 0.010	70 ± 10		7.25[a]	100	0.8 sec[c]
^{221}Ac	7.170 ± 0.010	∿ 2	52 ± 2msec			
	7.375 ± 0.010	10 ± 5				
	7.440 ± 0.015	20 ± 5		7.42[a]	30	
	7.645 ± 0.010	70 ± 10		7.63[a]	70	
^{217}Fr	8.315 ± 0.008	100	22 ± 5μsec	8.31[a]	100	
^{213}At	9.080 ± 0.012	100	0.11±0.02μsec	9.06[a]	100	
^{224}Pa chain						
^{224}Pa	7.49 ± 0.010	∿ 100	0.95±0.15sec			
	7.88 (?)					
	7.96 (?)					
^{220}Ac	7.61 ± 0.02	23±5	26.1 ± 0.5msec			
	7.68 ± 0.02	21±5				
	7.790± 0.010	13±2				
	7.850± 0.010	24±2				
	7.985± 0.010	4±2				

(continued)

Table II. continued

Nuclide	Present Results: α-Particle energy (MeV)	Present Results: Intensity %	Present Results: $T_{1/2}$	Previous Reports: α-Particle energy (MeV)	Previous Reports: Intensity %	Previous Reports: $T_{1/2}$
↓	8.005 ± 0.010	5 ± 3				
↓	8.060 ± 0.010	6 ± 1				
↓	8.195 ± 0.010	3 ± 1				
^{216}Fr	9.005 ± 0.012	100	0.70 ± 0.02μsec			
^{223}Pa chain						
^{223}Pa	8.005 ± 0.010	55 ± 5	6.5 ± 1.0 msec			
↓	8.195 ± 0.010	45 ± 5				
^{219}Ac	8.665 ± 0.010	100	7 ± 2μsec			
↓ ^{215}Fr	9.365 ± 0.015	100	< 0.5μsec			
^{222}Pa chain						
^{222}Pa	8.16		5.7 ± 0.5 msec			
↓	8.18	∿ 50				
↓	8.21					
↓	8.33	∿ 20				
↓	8.54	∿ 30				
^{218}Ac	9.205 ± 0.015		0.27 ± 0.04μsec			

[a]See Ref. 12.

[b]See Ref. 10.

[c]See Ref. 11.

Table III. Experimental and Predicted Q values (all values expressed in MeV)

	This Work		Predictions of Other Authors			
Nucleus	Experiment	Estimate	Myers *et al.*[a)]	Garvey *et al.*[b)]	Viola *et al.*[c)]	Zeldes *et al.*[d)]
^{225}Pa	7.400		8.460	7.53	7.41	7.370
^{224}Pa	7.650		8.689	7.98	7.82	7.776
^{223}Pa	8.375		8.931	8.38	8.42	8.144
^{222}Pa	8.72		9.159	8.90	8.97	8.511
^{221}Pa		9.19	9.401	9.49	9.31	8.913
^{220}Pa		9.70	9.629	10.26	9.77	9.408
^{219}Pa		10.06	9.871	10.89	10.00	9.979
^{218}Pa		9.70	8.364	9.94	-	9.342
^{221}Ac	7.810		8.176	7.59	-	7.709
^{220}Ac	8.38		8.412	8.07	-	8.099
^{219}Ac	8.870		8.662	8.70	-	8.523
^{218}Ac	9.415		8.897	9.36	9.46	9.040
^{217}Ac		9.87	9.147	9.98	9.70	9.633

(continued)

Table III. continued

	This Work		Predictions of Other Authors			
Nucleus	Experiment	Estimate	Myers *et al.*[a]	Garvey *et al.*[b]	Viola *et al.*[c]	Zeldes *et al.*[d]
^{217}Fr	8.495		7.898	8.47	8.460	8.315
^{216}Fr	9.205		8.141	9.17	9.30	8.855
^{215}Fr	9.575		8.399	9.76	9.586	9.471
^{213}At	9.285		7.626	9.05	9.380	9.306

[a] Ref. 16.

[b] Ref. 17.

[c] Ref. 18.

[d] Ref. 19

Table IV. Hindrance Factors for Alpha Decay

N	Nuclide	E_α (MeV)	$\log_{10}F$	N	Nuclide	E_α (MeV)	$\log_{10}F$
128	^{213}At	9.080	0.39	132	^{221}Ac	7.170	0.81
						7.375	0.79
129	^{216}Fr	9.005	0.33			7.440	0.81
						7.645	0.81
130	^{217}Fr	8.315	0.06				
				133	^{222}Ac	7.00	0.46
131	^{219}Ra	7.980	0.96				
		7.675	0.55	133	^{223}Th	7.315	0.71
						7.285	0.39
129	^{218}Ac	9.205	-0.14				
				131	^{221}Th	8.470	1.99
130	^{219}Ac	8.665	-0.13			8.145	0.81
						7.73	0.70
131	^{220}Ac	7.61	3.28				
		7.68	3.97	131	^{222}Pa	8.18	2.38
		7.790	3.92			8.33	1.85
		7.850	3.87			8.54	1.01
		7.985	1.68				
		8.005	1.66	132	^{223}Pa	8.005	1.09
		8.060	1.16			8.195	0.43
		8.195	0.84				
				133	^{224}Pa	7.49	0.64
				134	^{225}Pa	7.195	0.21
						7.245	0.43

FIGURE CAPTIONS

Fig. 1. Section of the chart of the nuclides indicating the group just above the 126 neutron and 82 proton shells with which this paper is concerned. Families of odd-Z alpha emitters on which new information is presented are outlined in black borders. The stable isotopes used as targets are shown by cross hatching.

Fig. 2. Alpha particle energy (for ground state transition) for isotopes of the elements bismuth to neptunium plotted versus neutron number. For isotopes with more than 126 neutrons only the odd-Z elements are shown. A comparable figure for the even-Z elements is given in Ref. 1.

Fig. 3. Schematic cut through center of cylindrical reaction cell. Central portion of cell is filled with helium at 2.2 atmospheres pressure supplied through He inlet at top of drawing. The cell is mounted in a vacuum chamber open to the beam pipe. Vacuum seal is made by O-rings represented by black dots. The windows are 4.5 mg/cm^2 Ni. The 1 cm flight path for recoiling nuclei corresponds to 5 cm^3 of He at a density of 0.4 mg/cm^3. He gas flows out of chamber via 0.4 mm diameter capillary, 6.5 cm long. Recoil nuclei collect on a plate positioned in front of an annular detector. The line marked degrader foils represents a set of aluminum absorbers mounted on a wheel and adjustable from outside the vacuum chamber.

Fig. 4. Schematic diagram of electronics used in Method I to study time correlation of alpha particles from a single detector. TAC stands for time-to-amplitude converter. The time sequence of pulse forms at points A, B, C, etc. in the diagram is displayed in the lower part of the figure.

A. Two linear (energy) signals.

B. The analogous time signals.

C. Gate signal generated if the start pulse is accepted by the TAC, i.e. if the TAC is not busy.

D. Gate signal, generated if the stop pulse is accepted by the TAC, i.e. if it has been proceeded by a (accepted) start pulse within the time range of the TAC.

E. The linear signal corresponding to the "start α" after passing first gate.

F. The same (start α) stretched for a time equal to the TAC time range.

G. Section of this stretched signal gated through to the analyzer by the valid stop signal D.

H. Linear signal corresponding to the "stop α" gated through to the analyzer by the valid stop signal (D).

J. The TAC output proportional to the time elapsed between the emission of the two α-particles (B).

Fig. 5. Schematic diagram of electronics used in the Method II to study time correlation of alpha particles from a single detector.

The time sequence of pulse forms at points A, B, and C in the diagram is displayed in the lower part of the figure.

A. Two linear (energy) signals added in the linear amplifier.

B. The analogous time signals.

C. The TAC output proportional to the time elapsed between the emission of the two α-particles.

Fig. 6. Alpha-particle spectra of products of the $^{209}Bi + ^{22}Ne$ reaction for two bombarding energies. Spectra recorded over a 30 minute period in the 20 msec intervals between 4 msec beam pulses.

Fig. 7. Yield of individual products as a function of bombardment energy in the $^{209}Bi + ^{22}Ne$ reaction.

Fig. 8. Alpha-particle spectra of products of the $^{208}Pb + ^{19}F$ reaction for two bombarding energies. Spectra recorded over a 30 minute period in the 20 msec intervals between 4 msec beam pulses.

Fig. 9. Yield of individual products as a function of bombardment energy in the $^{208}Pb + ^{19}F$ reaction.

Fig. 10. Alpha-particle spectra of products of the $^{205}Tl + ^{22}Ne$ reaction at three bombarding energies. Spectra recorded over a 30 minute period in the 20 msec intervals between 4 msec beam pulses.

Fig. 11. Yield of individual products as a function of bombardment energy in the $^{205}Tl + ^{22}Ne$ reaction.

Fig. 12. Alpha spectra of products isolated from the reaction of ^{208}Pb with 115 MeV ^{19}F ions with data taken by TAC technique I described in Sec. II E. The TAC cycle time was 25 μsec. (a) unsorted start spectrum (b) unsorted stop spectrum (c) start spectrum of ^{221}Ac peaks obtained in data sort with windows B and C set on ^{217}Fr (8.31 MeV) and ^{213}At (9.08 MeV) in stop spectrum (d) stop spectrum of ^{217}Fr and ^{213}At obtained from data sort with window A set on ^{221}Ac peaks. The small ^{216}Rn peak at 8.05 MeV is due to a trace of ^{220}Ra (7.45 MeV) in the start spectrum.

Fig. 13. Half life of ^{217}Fr obtained from time parameter information derived from data sort with window A set on start pulses and window B and C set on stop pulses (see Fig. 12).

Fig. 14. Alpha sum spectrum taken by TAC method II (described in Sec. IIE) on products isolated from the interaction of 100 MeV ^{19}F with ^{208}Pb. The TAC range was 3 μsec. Peaks from the following mother-daughter pairs appear in the spectrum: ^{220}Ac + ^{216}Fr, ^{217}Fr + ^{213}At, and ^{219}Ac + ^{215}Fr. The position and length of the arrows shows the expected location and relative intensity (linear scale) of the sum peaks computed from the complexity in the α-groups from the mother and daughter. Windows A and B were used in a sort of the data with the MULTIS program to select time parameter information characteristic of ^{216}Fr and ^{213}At, respectively. (See Fig. 15.)

Fig. 15. Half life of ^{216}Fr from time parameter associated with α-sum events falling within window A of Fig. 14. Half life of ^{213}At from similar sort of data with α-sum energy specified by window B in Fig. 14.

Fig. 16. Determination of ^{213}At half life in an experiment similar to that described in the captions to Fig. 14 and 15 except that the TAC range was 1 μsec.

Fig. 17. ^{220}Ac alpha groups observed in the products of the ^{208}Pb + ^{15}N reaction at a beam energy of 75 MeV. Counts registered for 20 msec periods between 4 msec beam bursts. Total time about 20 minutes. Beam level about 0.3 μamp. The tailing on the high-energy side of the ^{216}Fr peak is caused by partial overlap of pulses from the 0.7 μsec ^{216}Fr with ^{220}Ac parent pulses.

Fig. 18. Half life of ^{220}Ac determined from observed decay of 9.005 MeV ^{216}Fr α-peak. Sample prepared by ^{208}Pb + ^{15}N reaction.

Fig. 19. Results of measurements on products of ^{208}Pb + 75 MeV ^{15}N by TAC method I. Start spectrum from MULTIS program sort imposing the requirement that stop pulse have amplitude corresponding to 9.005 MeV ^{216}Fr. 0.2 μsec shaping constants for amplifier. TAC range was 3 μsec with 0.4 μsec delay on start pulse. The ^{216}Fr pulses represent accidental coincidences. Because

^{216}Fr and ^{212}At are of comparable intensity in the singles spectrum (Fig. 17) we may expect a contribution in the TAC spectrum at 7.67 MeV comparable to the spurious ^{216}Fr peak.

Fig. 20. Half life of ^{216}Fr from MULTIS program sort of TAC experiment data. This time parameter information is associated with the energy information displayed in Fig. 19.

Fig. 21. Alpha particle spectrum of products from the reaction of 108 MeV ^{20}Ne ions on ^{209}Bi. Spectra recorded over a 30 minute period in the 20 msec intervals between 4 msec beam pulses.

Fig. 22. Yield of individual products of the ^{209}Bi + ^{20}Ne reaction as a function of the bombardment energy.

Fig. 23. Alpha-particle spectrum of products of ^{206}Pb + ^{19}F reaction. Data recorded over a 2 hour period in the 20 msec intervals between 4 msec beam pulses. The ^{224}Pa decay chain members are present in this spectrum because of the 1.5% ^{208}Pb content in the target.

Fig. 24. Alpha-particle spectrum of products of the ^{209}Bi + ^{16}O reaction. Data recorded over a 2 hour period in the 20 msec intervals between 4 msec beam pulses.

Fig. 25. Yield of individual products as a function of bombardment energy in the ^{209}Bi + ^{16}O reaction.

Fig. 26. Alpha-particle energies of ground state transitions for the isotones N = 128 to N = 136 plotted versus proton number.

	124	125	126	127	128	129	130	131	132	133	134	135	136	137	138
93													Np 229	Np 230	Np 231
92												U 227	U 228	U 229	U 230
91			Pa 217					Pa 222	Pa 223	Pa 224	Pa 225	Pa 226	Pa 227	Pa 228	Pa 229
90	Th 214	Th 215	Th 216	Th 217			Th 220	Th 221	Th 222	Th 223	Th 224	Th 225	Th 226	Th 227	Th 228
89	Ac 213	Ac 214	Ac 215	Ac 216		Ac 218	Ac 219	Ac 220	Ac 221	Ac 222	Ac 223	Ac 224	Ac 225	Ac 226	Ac 227
88	Ra 212	Ra 213	Ra 214	Ra 215	Ra 216	Ra 217	Ra 218	Ra 219	Ra 220	Ra 221	Ra 222	Ra 223	Ra 224	Ra 225	Ra 226
87	Fr 211	Fr 212	Fr 213	Fr 214	Fr 215	Fr 216	Fr 217	Fr 218	Fr 219	Fr 220	Fr 221	Fr 222	Fr 223	Fr 224	Fr 225
86	Rn 210	Rn 211	Rn 212	Rn 213	Rn 214	Rn 215	Rn 216	Rn 217	Rn 218	Rn 219	Rn 220	Rn 221	Rn 222	Rn 223	Rn 224
85	At 209	At 210	At 211	At 212	At 213	At 214	At 215	At 216	At 217	At 218	At 219				
84	Po 208	Po 209	Po 210	Po 211	Po 212	Po 213	Po 214	Po 215	Po 216	Po 217	Po 218				
83	Bi 207	Bi 208	Bi 209	Bi 210	Bi 211	Bi 212	Bi 213	Bi 214	Bi 215						
82	Pb 206	Pb 207	Pb 208	Pb 209	Pb 210	Pb 211	Pb 212	Pb 213	Pb 214						
81	Tl 205	Tl 206	Tl 207	Tl 208	Tl 209	Tl 210									

XBL701-2166

Fig. 1

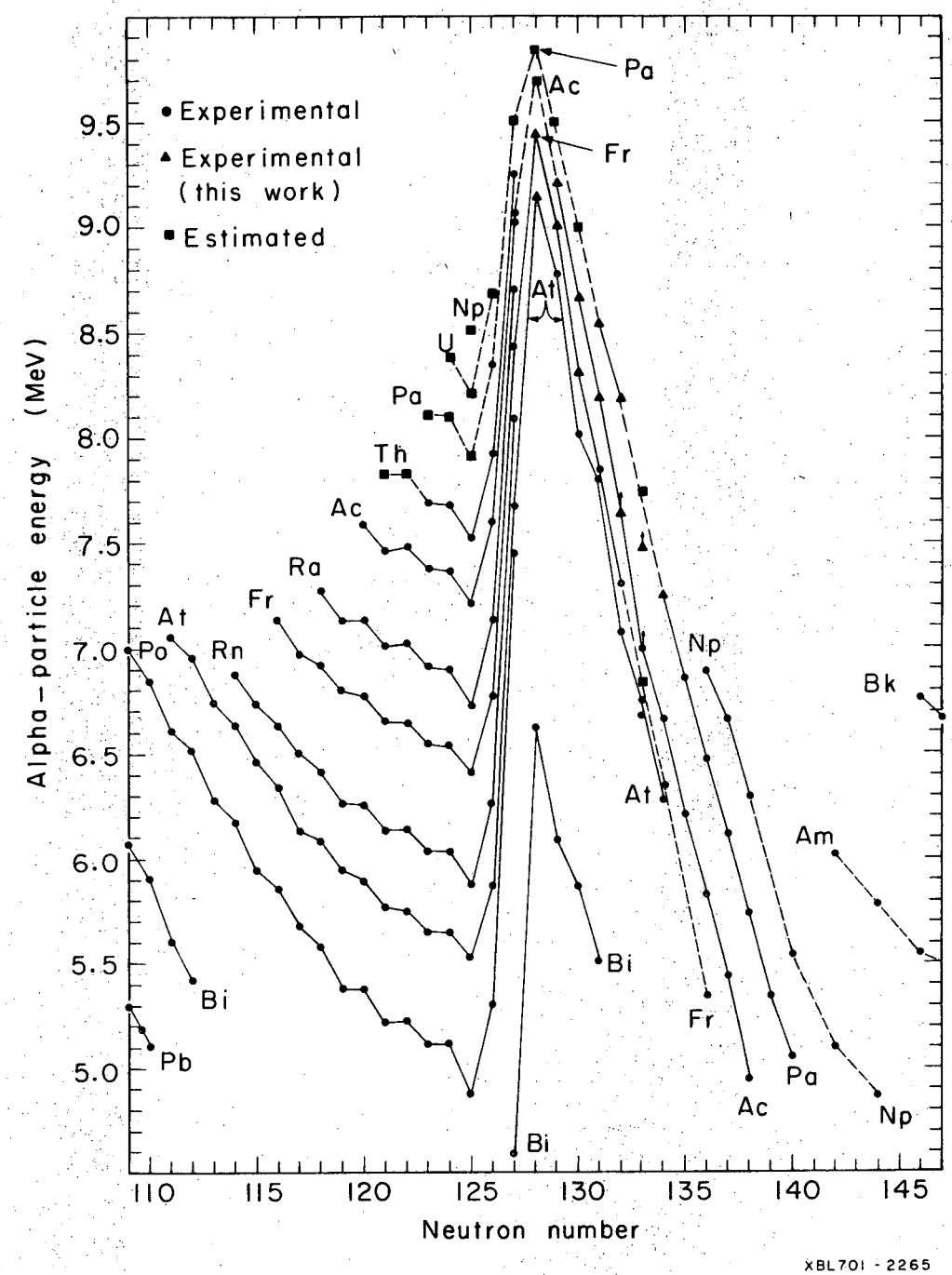
• Experimental
▲ Experimental (this work)
■ Estimated
Alpha-particle energy (MeV)
Neutron number
9.5
9.0
8.5
8.0
7.5
7.0
6.5
6.0
5.5
5.0
110
115
120
125
130
135
140
145
Pa
Ac
Fr
At
Np
U
Pa
Th
Ac
Ra
Fr
At
Po
Rn
Bi
Pb
Bi
Np
Bk
At
Am
Bi
Fr
Pa
Ac
Np
XBL701-2265

Fig. 2

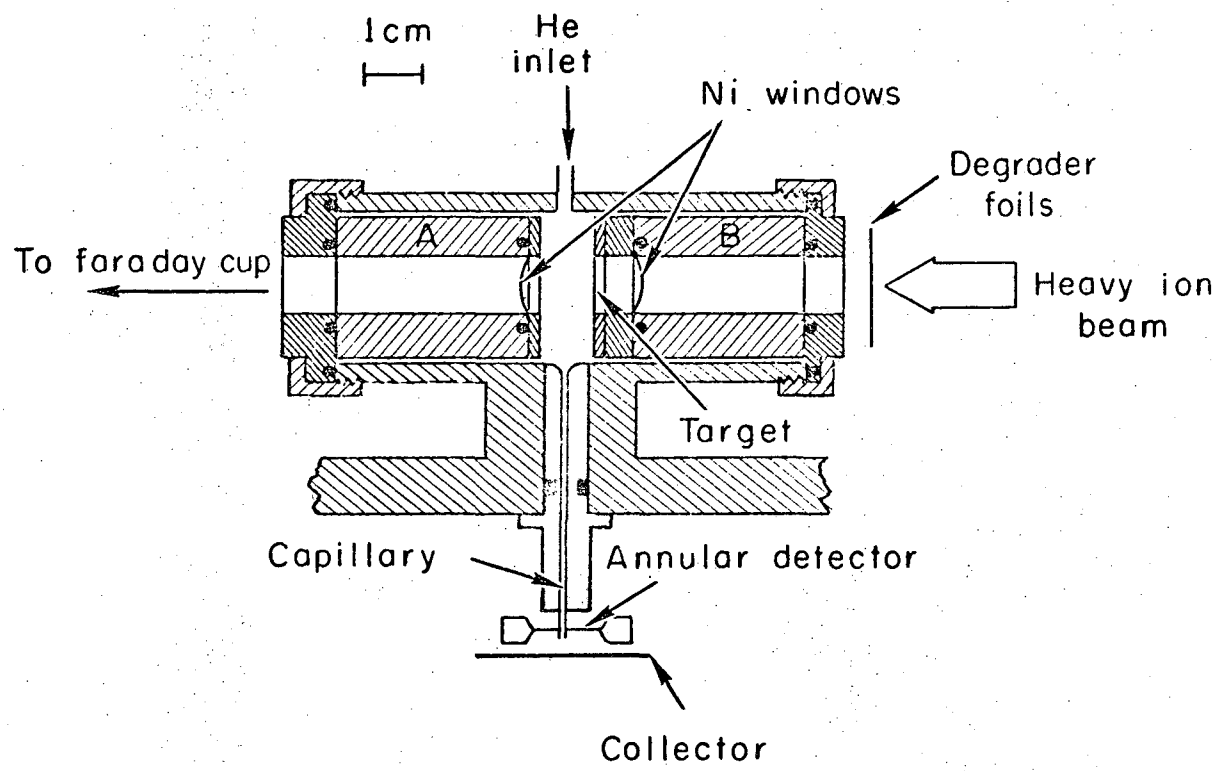

XBL701-2242

Fig. 3

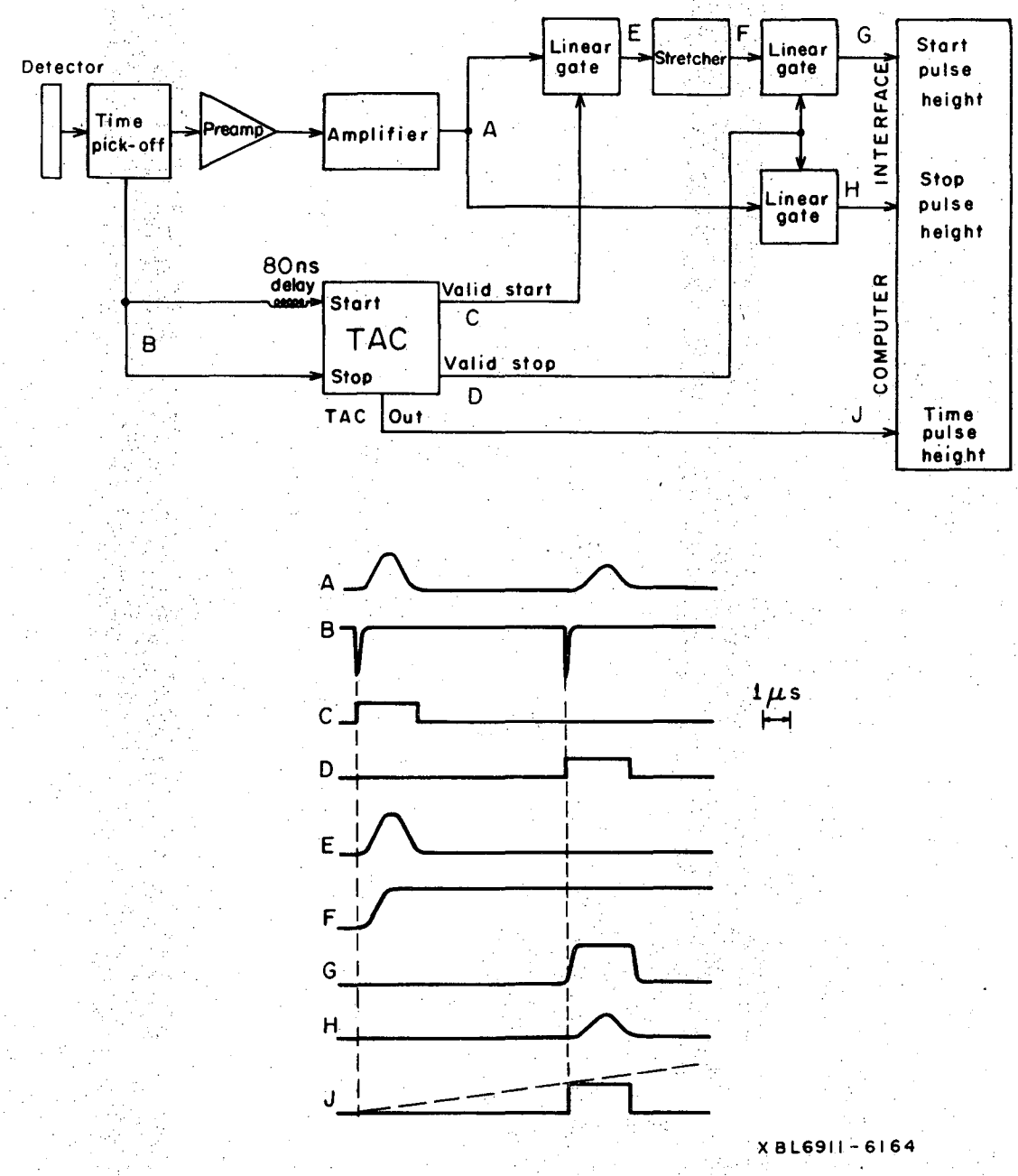
Detector
Time pick-off
Preamp
Amplifier
A
Linear gate
E
Stretcher
F
Linear gate
G
Linear gate
H
INTERFACE
COMPUTER
Start pulse height
Stop pulse height
Time pulse height
80ns delay
Start
TAC
Stop
Valid start
C
Valid stop
D
B
TAC Out
J
A
B
C
D
E
F
G
H
J
1 μs
XBL6911-6164

Fig. 4

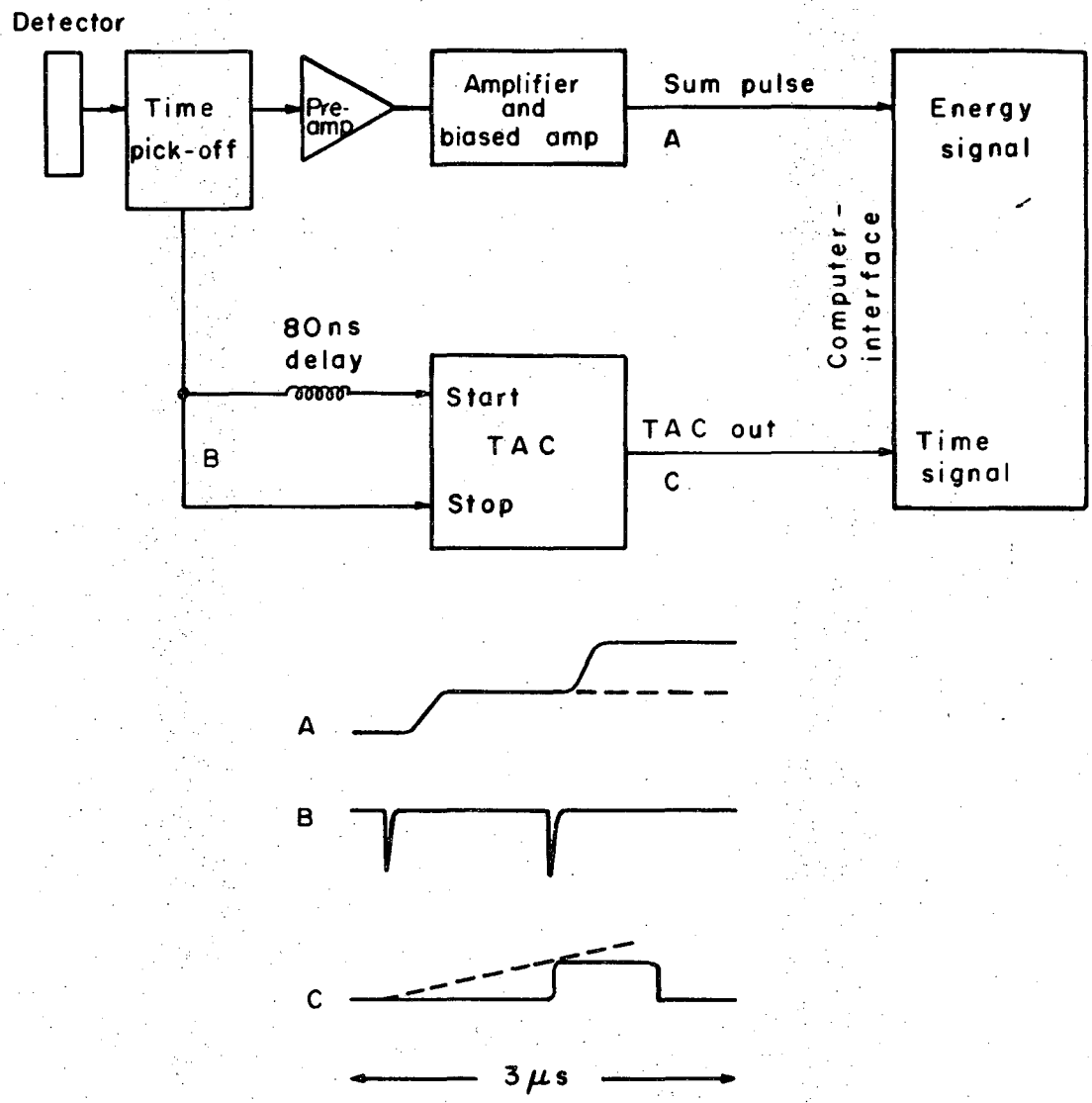

XBL701-2055

Fig. 5

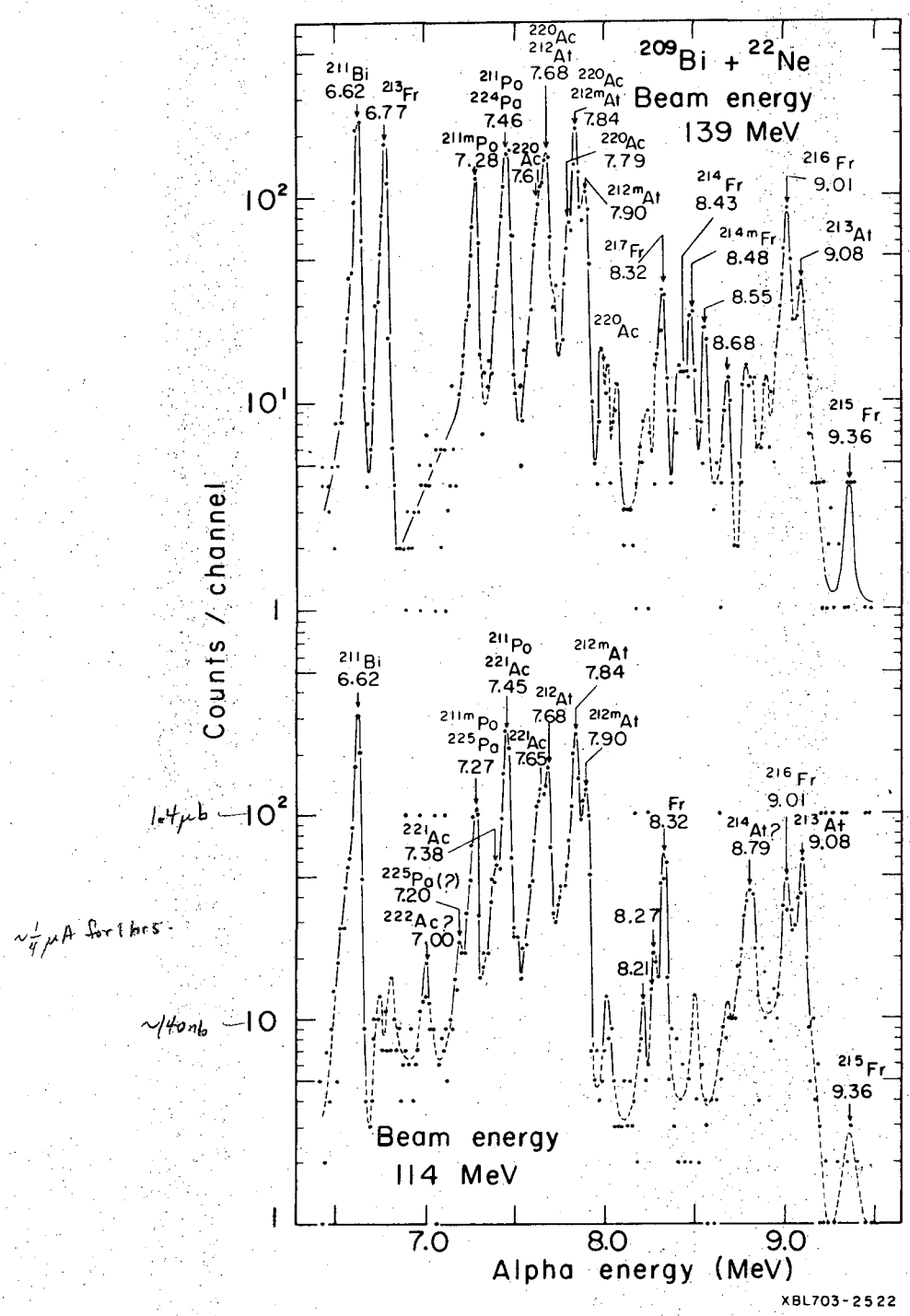
209Bi + 22Ne
Beam energy
139 MeV
211Bi 6.62
213Fr 6.77
211Po 224Po 7.46
211mPo 7.28
220Ac 212At 7.68
220Ac 7.61
220Ac 212mAt 7.84
220Ac 7.79
212mAt 7.90
217Fr 8.32
220Ac
214Fr 8.43
214mFr 8.48
8.55
8.68
216Fr 9.01
213At 9.08
215Fr 9.36
Counts / channel
211Bi 6.62
211Po 221Ac 7.45
212mAt 7.84
212At 7.68
211mPo 225Po 7.27
221Ac 7.65
212mAt 7.90
221Ac 7.38
225Po(?) 7.20
222Ac? 7.00
Fr 8.32
8.27
8.21
214At? 8.79
216Fr 9.01
213At 9.08
215Fr 9.36
1.4μb
~1/4 μA for 1 hrs.
~140nb
Beam energy
114 MeV
7.0
8.0
9.0
Alpha energy (MeV)
XBL703-2522

Fig. 6

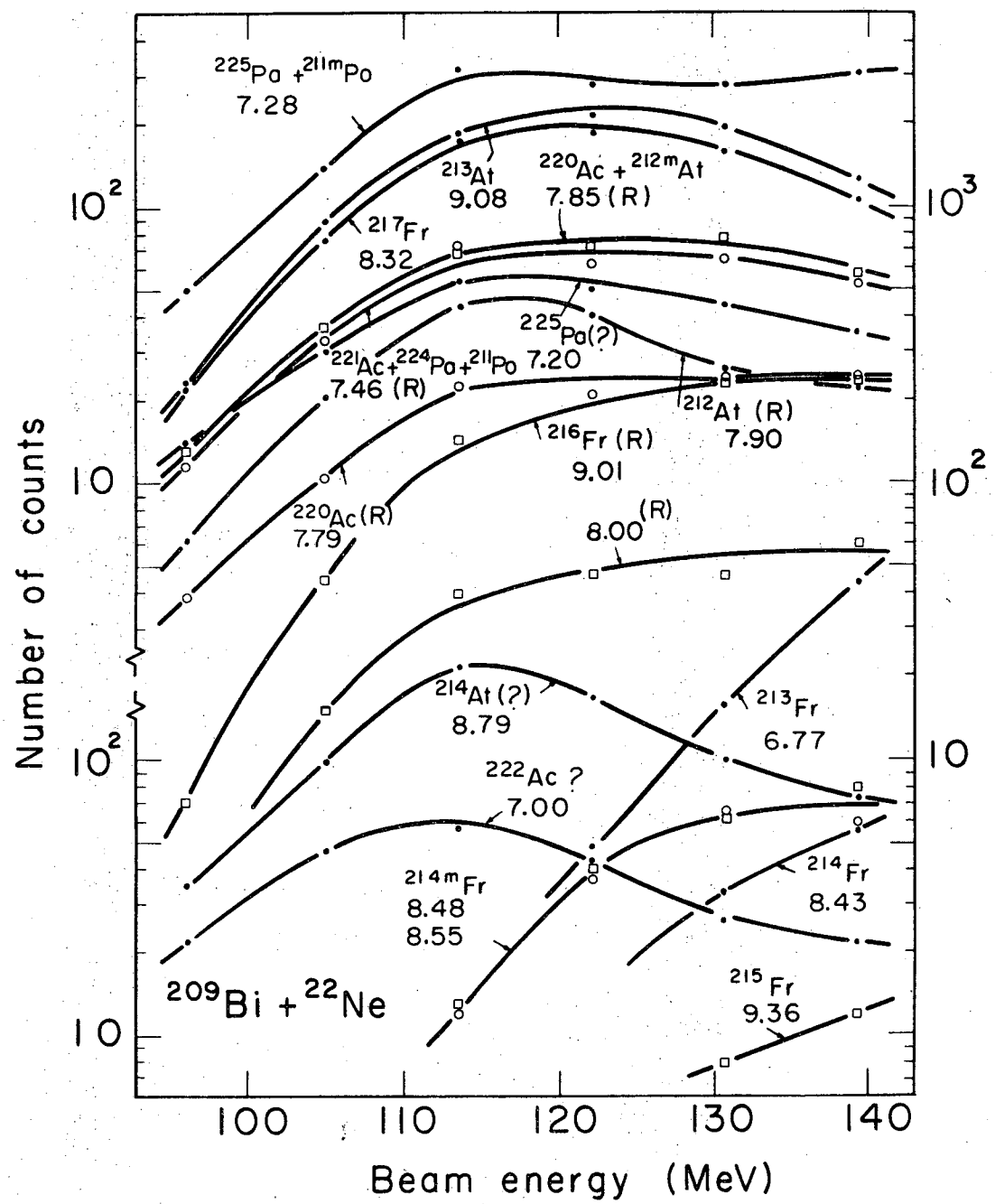
225Pa + 211mPo
7.28
213At
9.08
220Ac + 212mAt
7.85 (R)
217Fr
8.32
225Pa(?)
221Ac+224Pa+211Po 7.20
7.46 (R)
212At (R)
7.90
216Fr (R)
9.01
220Ac(R)
7.79
8.00(R)
214At (?)
8.79
213Fr
6.77
222Ac ?
7.00
214mFr
8.48
8.55
214Fr
8.43
215Fr
9.36
209Bi + 22Ne
Number of counts
Beam energy (MeV)
100
110
120
130
140
10
10²
10³
XBL703-2521

Fig. 7

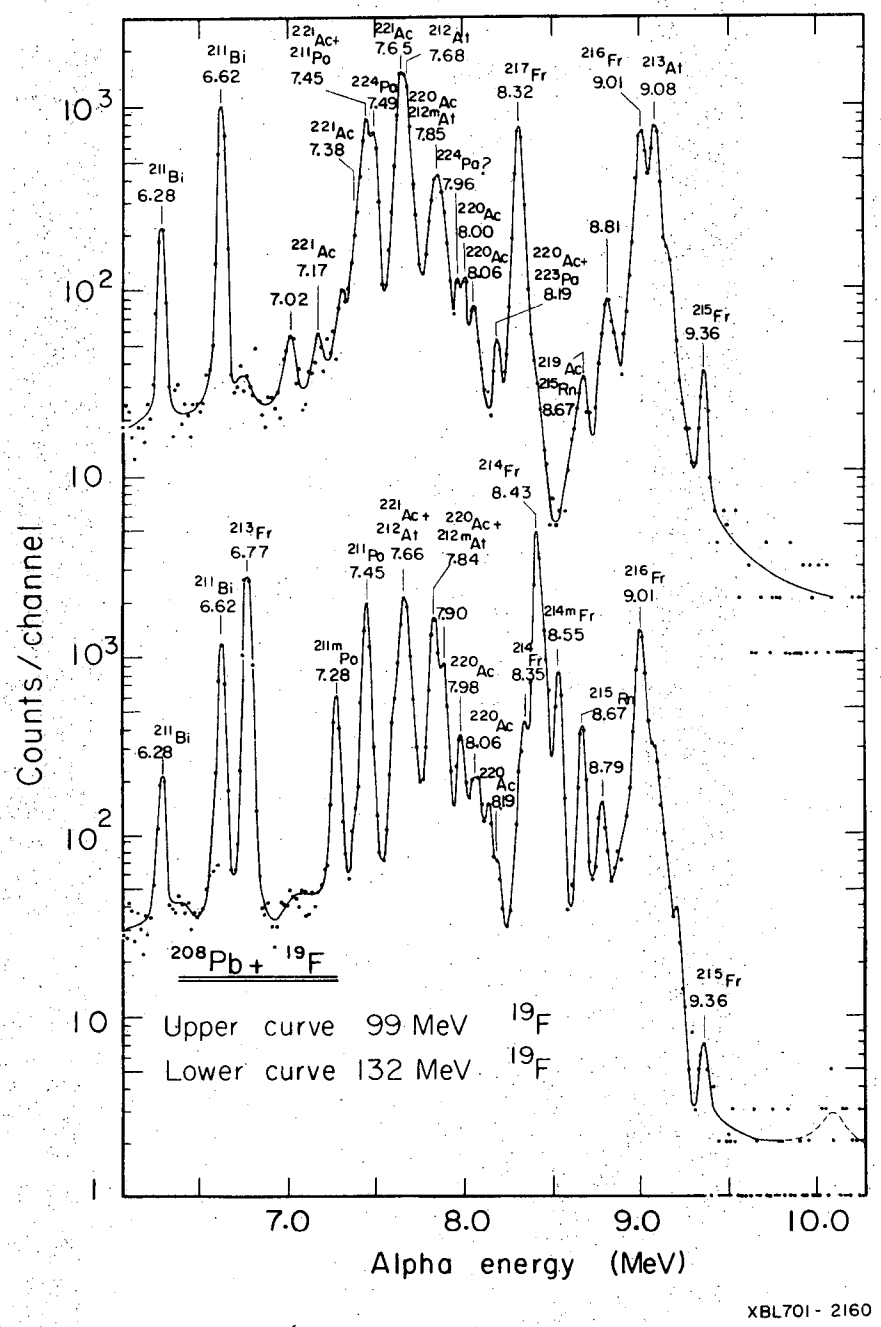
Counts/channel
Alpha energy (MeV)
$^{208}Pb + ^{19}F$
Upper curve 99 MeV ^{19}F
Lower curve 132 MeV ^{19}F
^{211}Bi 6.28
^{211}Bi 6.62
^{221}Ac 7.02
^{221}Ac 7.17
^{221}Ac 7.38
^{221}Ac + ^{211}Po 7.45
^{224}Pa 7.49
^{221}Ac 7.65
^{212}At 7.68
^{220}Ac ^{212m}At 7.85
^{224}Pa? 7.96
^{220}Ac 8.00
^{220}Ac 8.06
^{220}Ac + ^{223}Pa 8.19
^{217}Fr 8.32
^{219}Ac ^{215}Rn 8.67
8.81
^{216}Fr 9.01
^{213}At 9.08
^{215}Fr 9.36
^{214}Fr 8.43
^{213}Fr 6.77
^{211}Po 7.45
^{221}Ac + ^{212}At 7.66
^{220}Ac + ^{212m}At 7.84
7.90
^{211m}Po 7.28
^{220}Ac 7.98
^{220}Ac 8.06
^{220}Ac 8.19
^{214}Fr 8.35
^{214m}Fr 8.55
^{215}Rn 8.67
8.79
^{216}Fr 9.01
^{215}Fr 9.36
XBL701 - 2160

Fig. 8

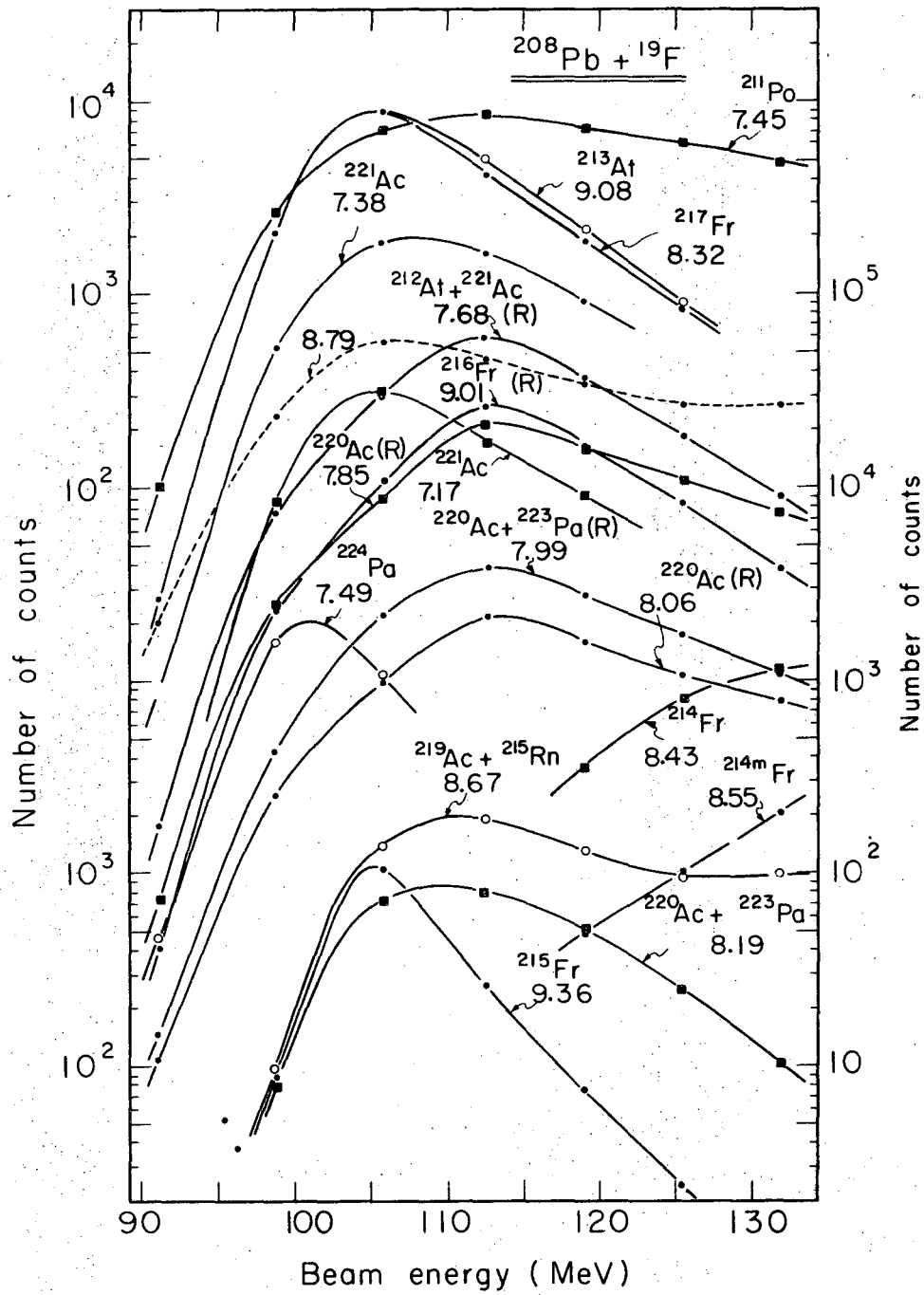
208Pb + 19F
211Po
7.45
213At
9.08
217Fr
8.32
221Ac
7.38
212At + 221Ac
7.68 (R)
8.79
216Fr (R)
9.01
220Ac(R)
7.85
221Ac
7.17
220Ac + 223Pa(R)
7.99
224Pa
7.49
220Ac (R)
8.06
214Fr
8.43
214mFr
8.55
219Ac + 215Rn
8.67
220Ac + 223Pa
8.19
215Fr
9.36
Number of counts
Number of counts
Beam energy (MeV)
90
100
110
120
130
XBL701-2162

Fig. 9

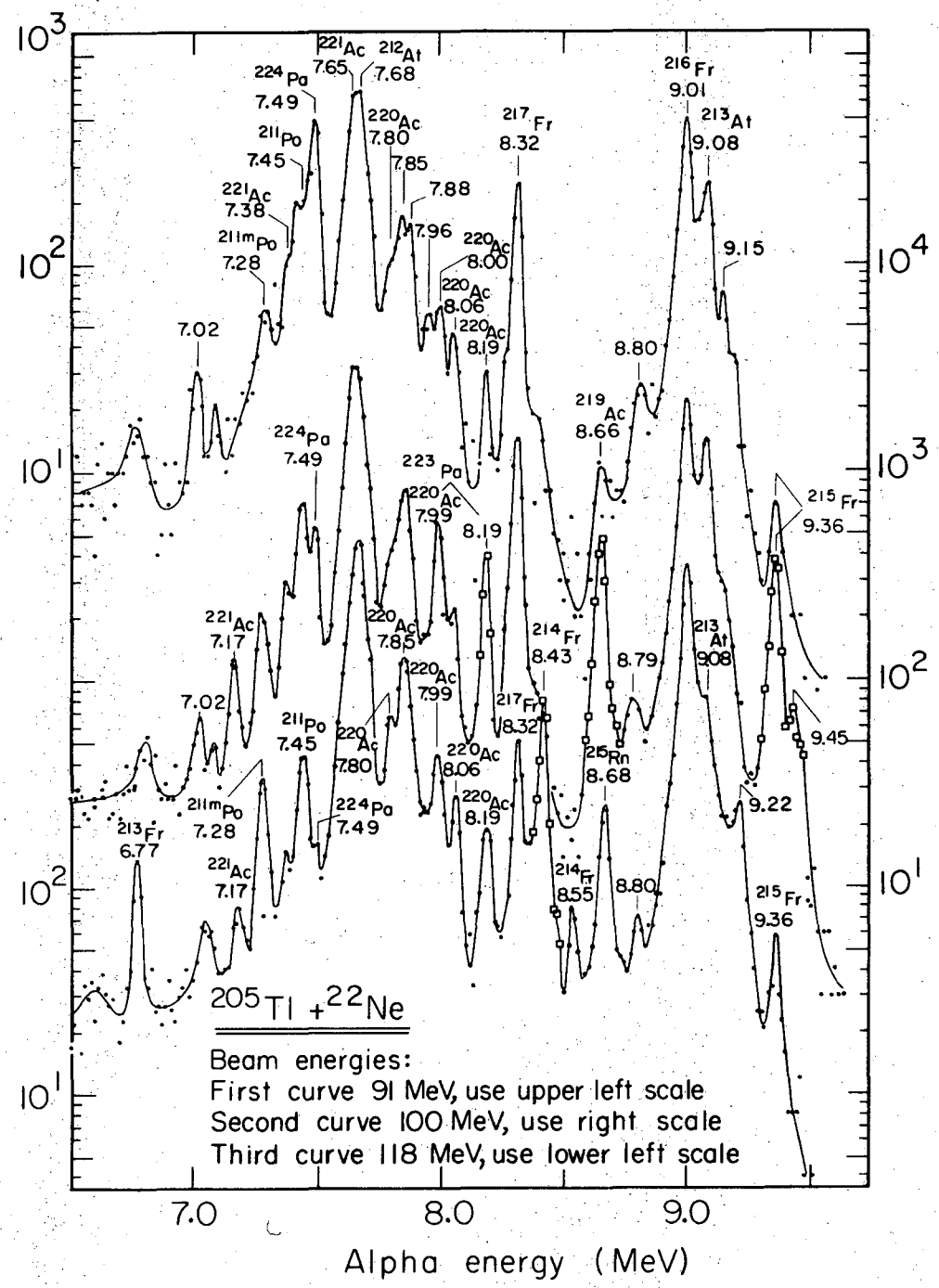

XBL701-2157

Fig. 10

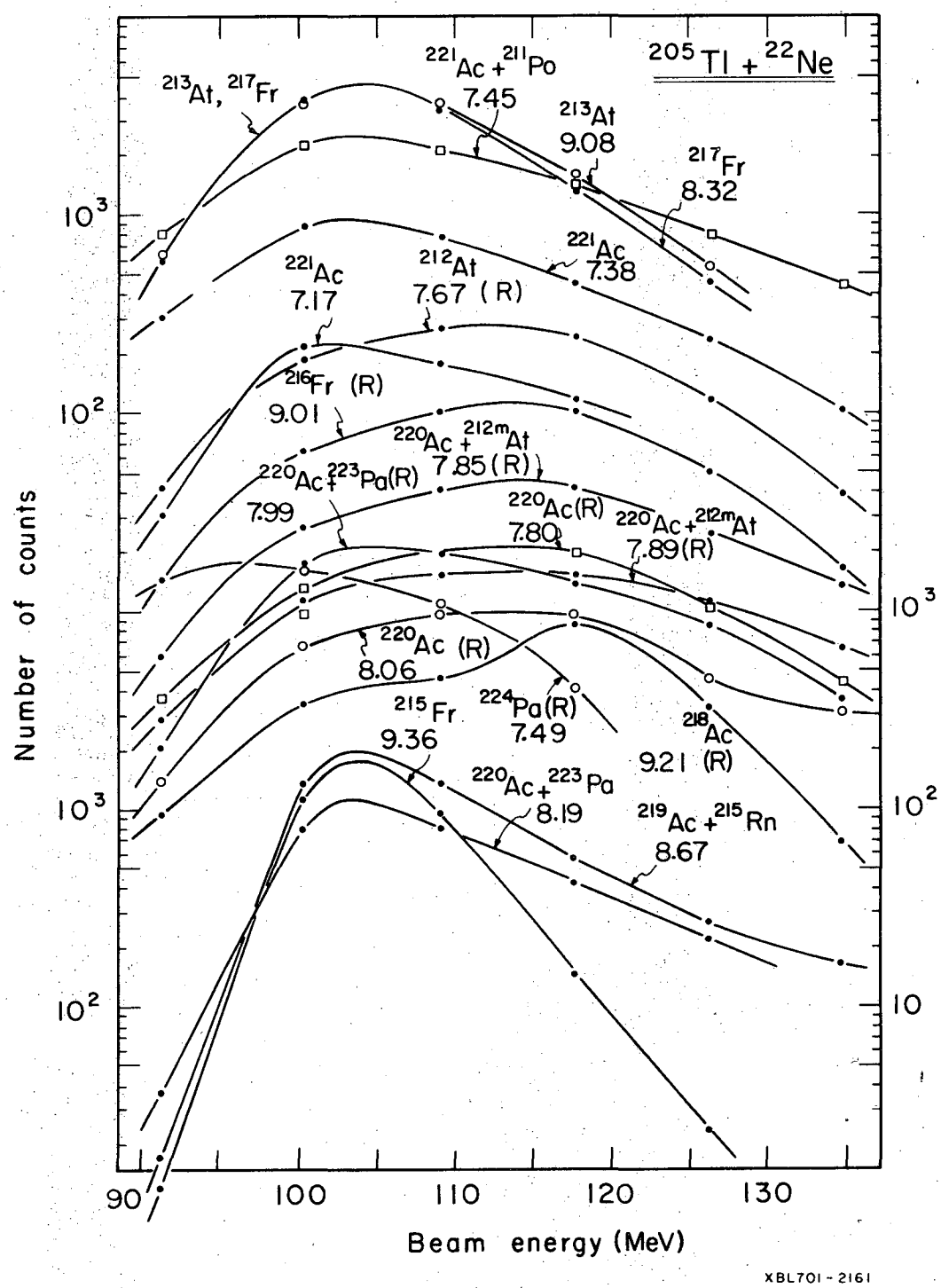
205Tl + 22Ne
213At, 217Fr
221Ac + 211Po
7.45
213At
9.08
217Fr
8.32
221Ac
7.38
221Ac
7.17
212At
7.67 (R)
216Fr (R)
9.01
220Ac + 212mAt
7.85 (R)
220Ac + 223Pa(R)
7.99
220Ac(R)
7.80
220Ac + 212mAt
7.89(R)
220Ac (R)
8.06
224Pa(R)
7.49
215Fr
9.36
218Ac
9.21 (R)
220Ac + 223Pa
8.19
219Ac + 215Rn
8.67
Number of counts
Beam energy (MeV)
90
100
110
120
130
10
XBL701-2161

Fig 11

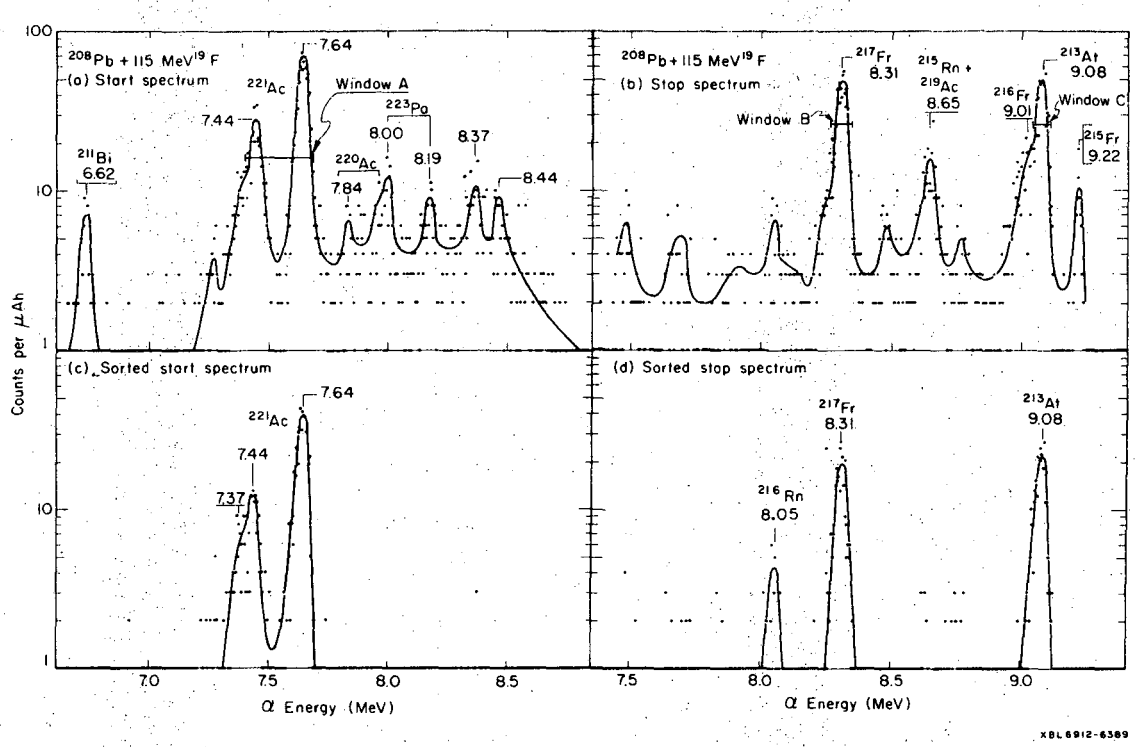
208Pb + 115 MeV 19F
(a) Start spectrum
211Bi 6.62
221Ac
7.44
7.64
Window A
223Pa
8.00
220Ac
7.84
8.19
8.37
8.44
208Pb + 115 MeV 19F
(b) Stop spectrum
Window B
217Fr 8.31
215Rn + 219Ac 8.65
216Fr 9.01
213At 9.08
Window C
215Fr 9.22
(c) Sorted start spectrum
7.37
7.44
221Ac
7.64
(d) Sorted stop spectrum
216Rn 8.05
217Fr 8.31
213At 9.08
Counts per μAh
100
10
1
7.0
7.5
8.0
8.5
9.0
α Energy (MeV)
XBL 6912-6389

Fig. 12

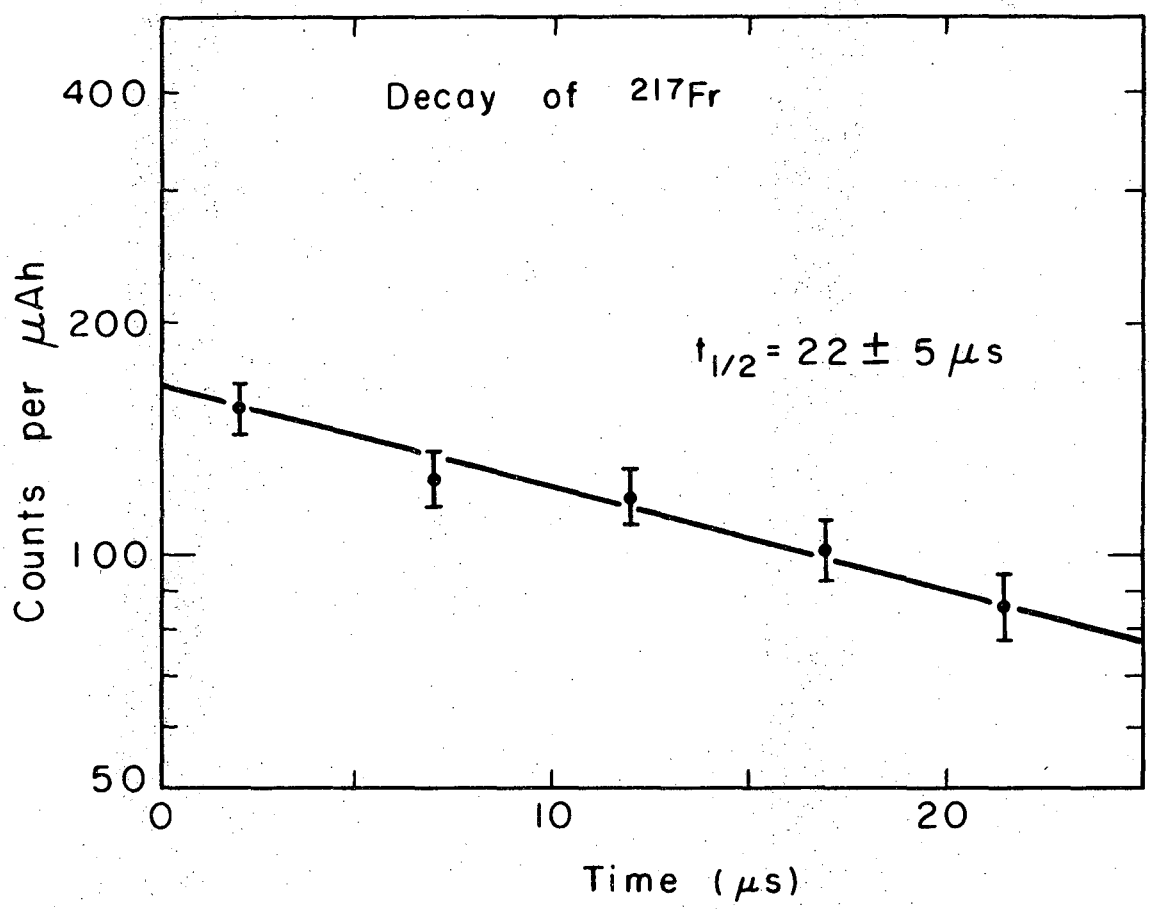

XBL701-2052

Fig. 13

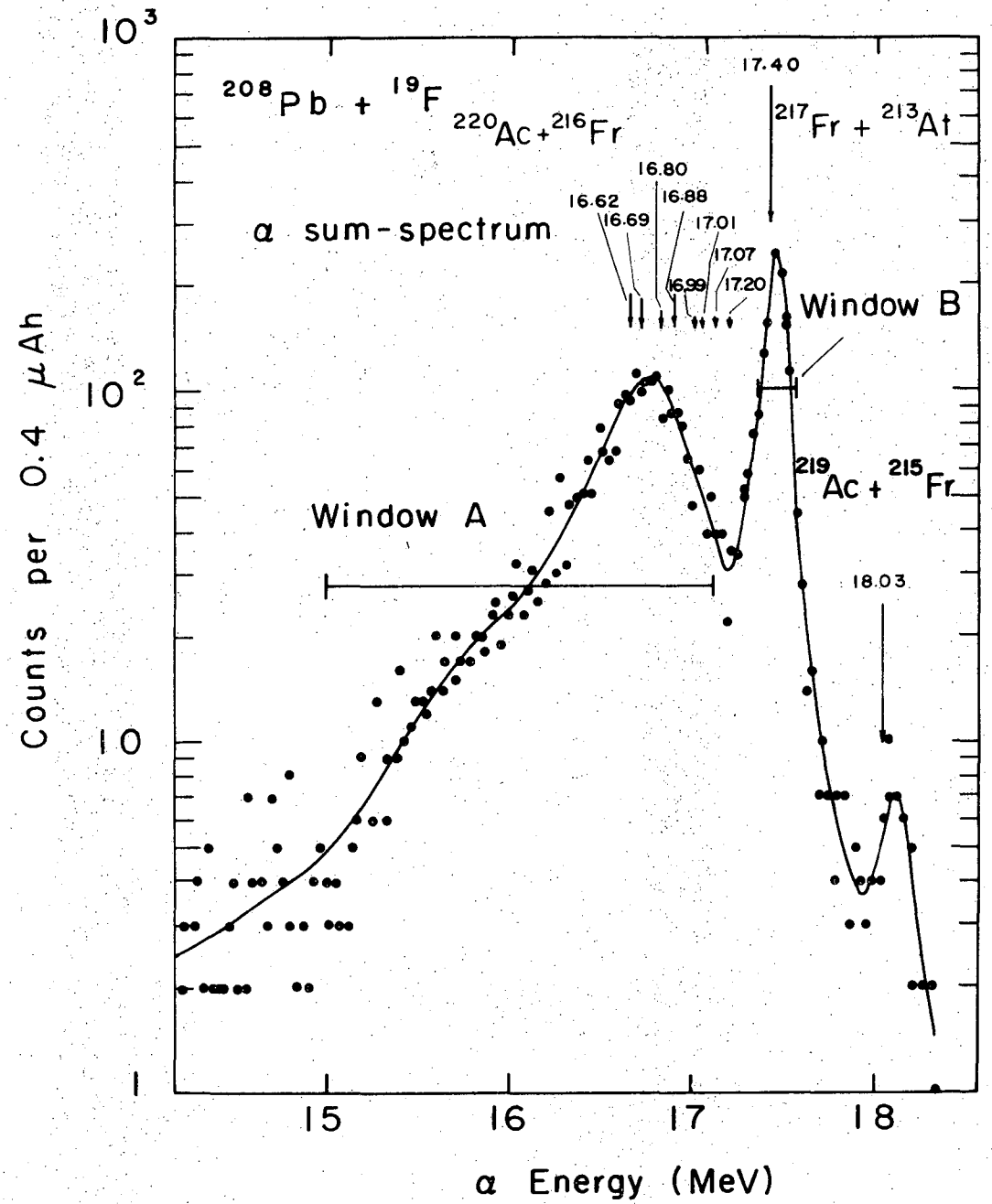

X BL701 - 2054

Fig. 14

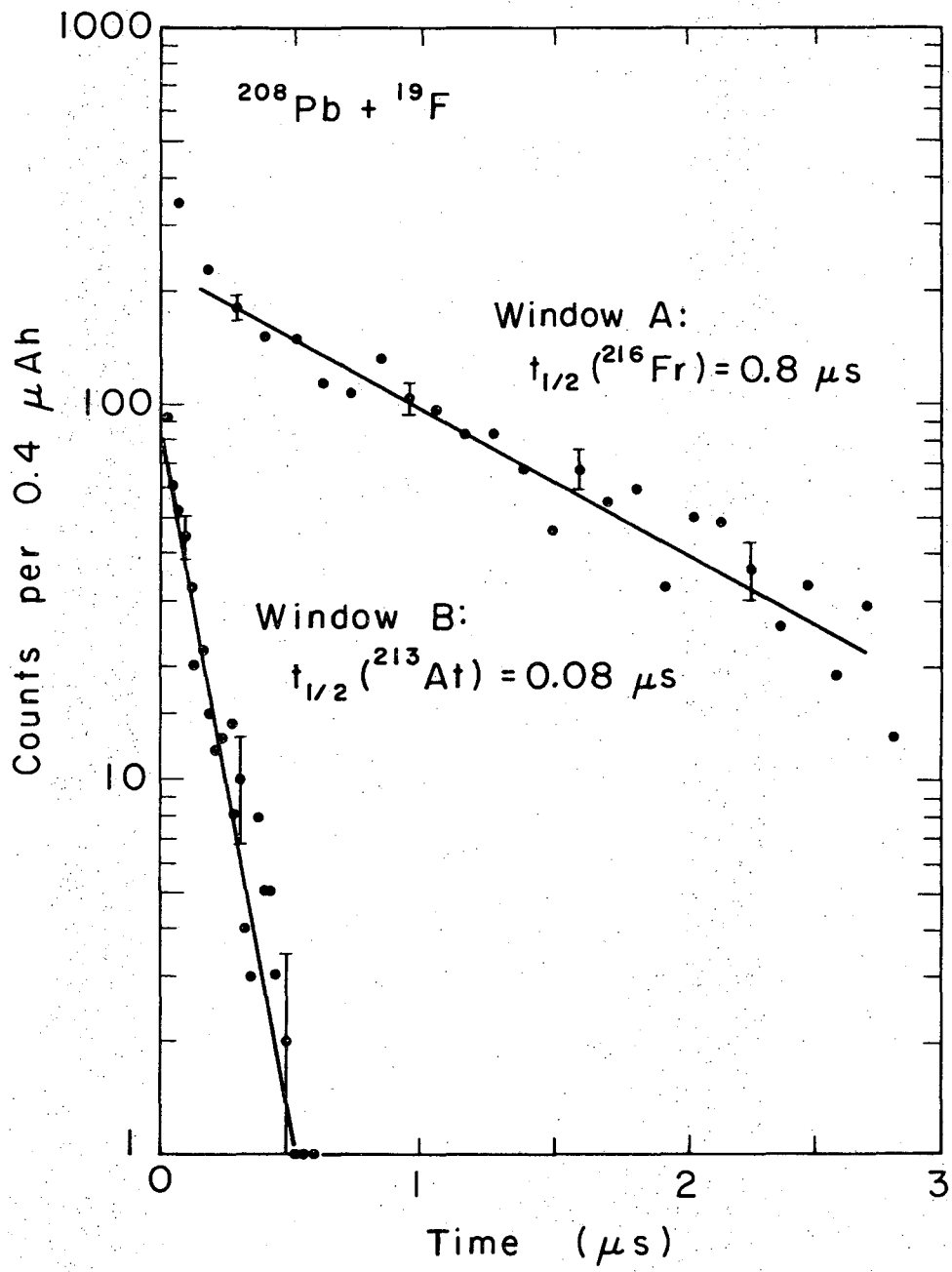

XBL701-2053

Fig. 15

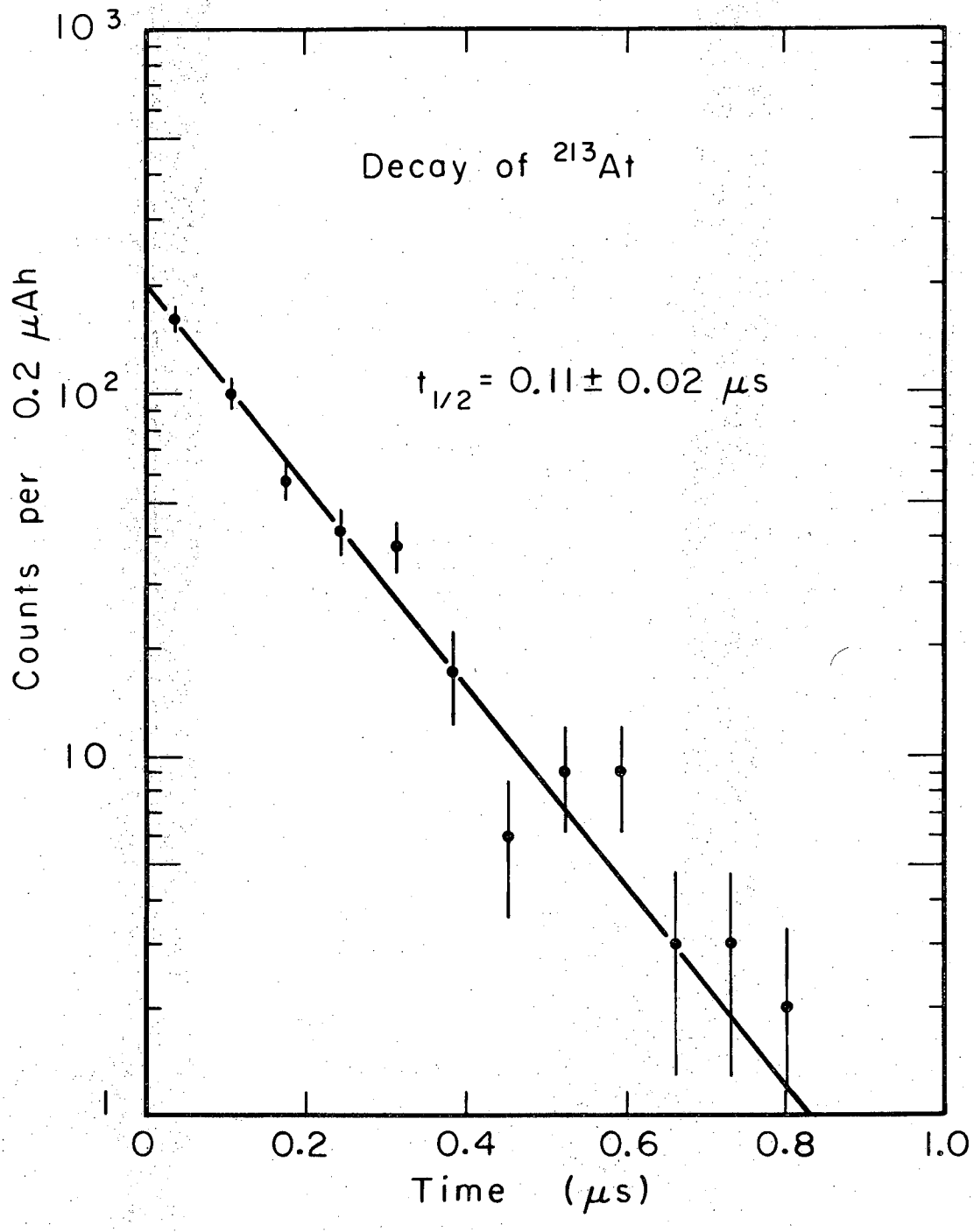

XBL 701 - 2163

Fig. 16

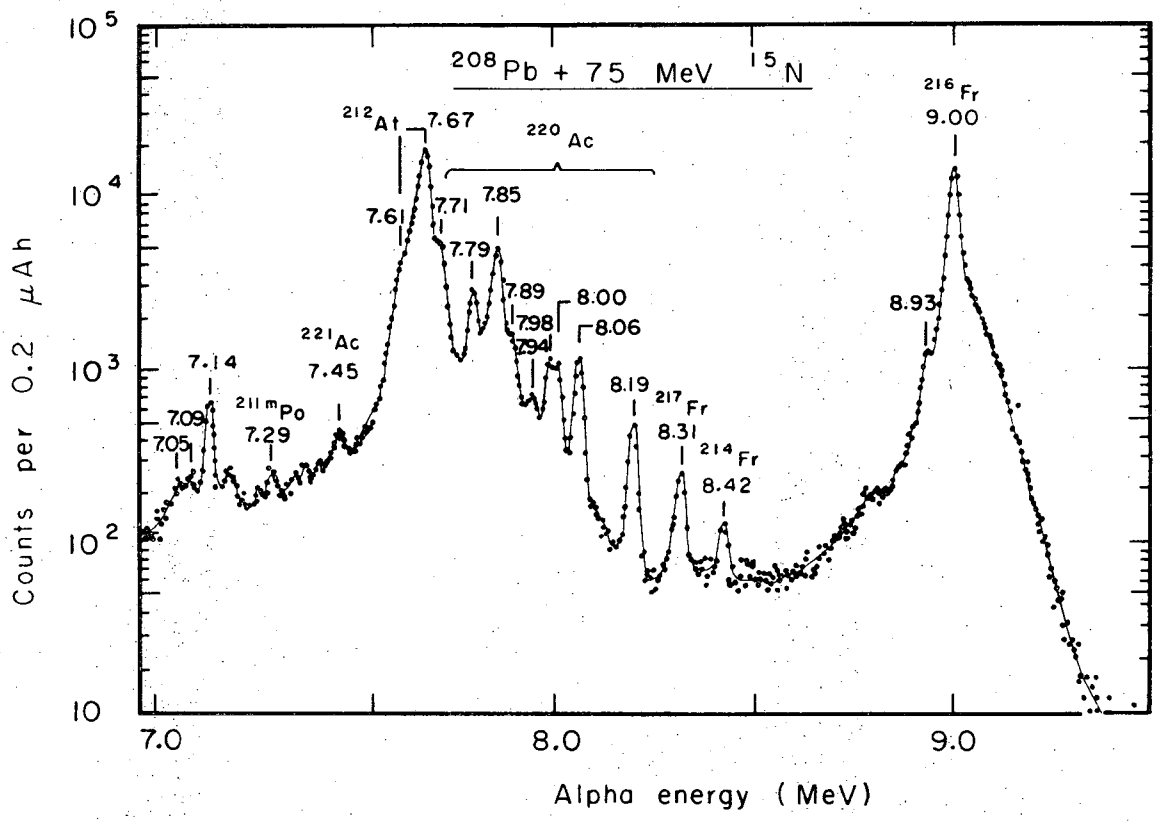
208Pb + 75 MeV 15N
212At
7.67
220Ac
7.61
7.71
7.85
7.79
7.89
8.00
8.06
7.98
7.94
221Ac
7.45
7.14
211mPo
7.29
7.09
7.05
8.19
217Fr
8.31
214Fr
8.42
216Fr
9.00
8.93
Counts per 0.2 μAh
Alpha energy (MeV)
XBL701 - 2165

Fig. 17

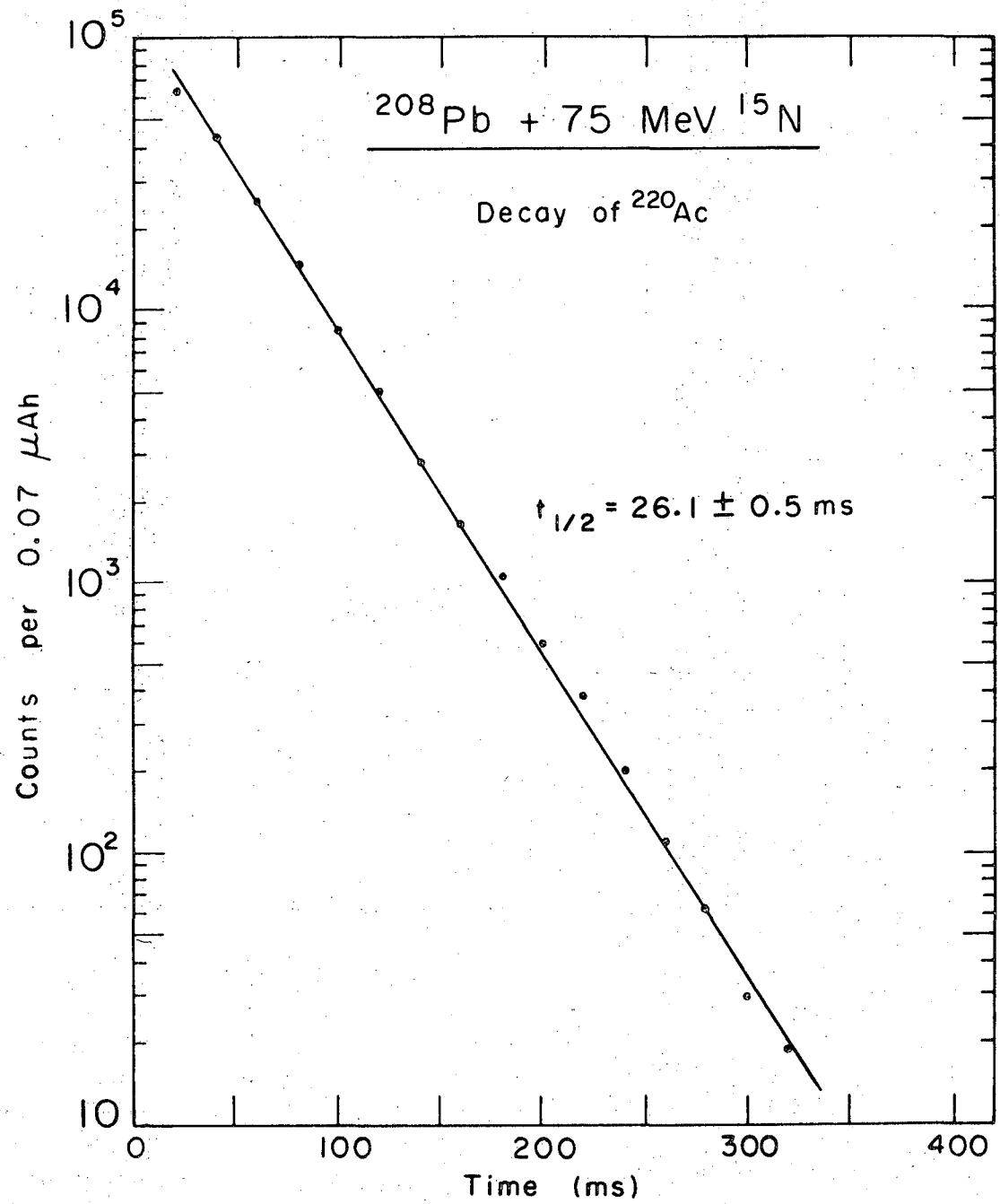

XBL 703-2428

Fig. 18

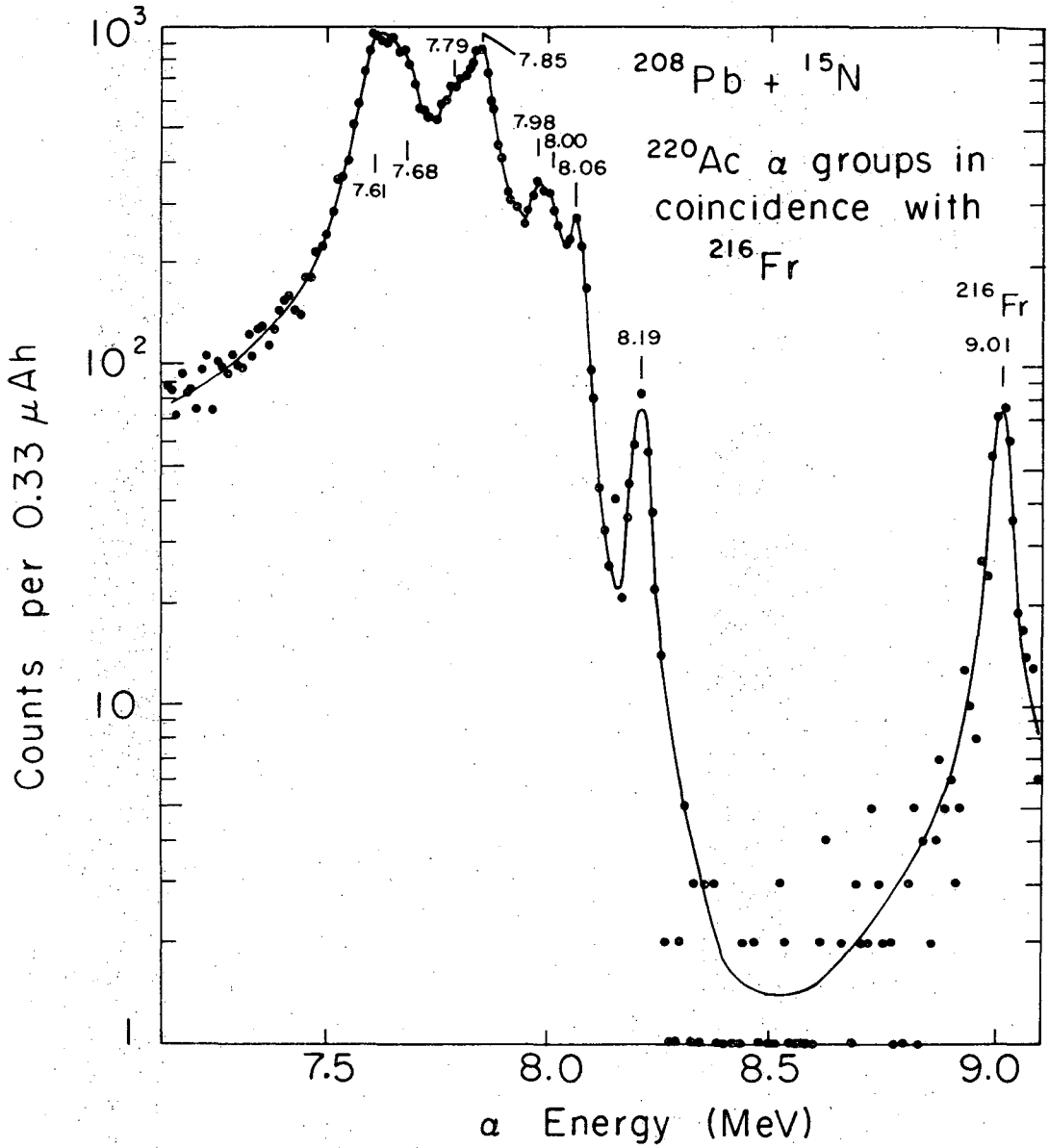

XBL701-2056

Fig. 19

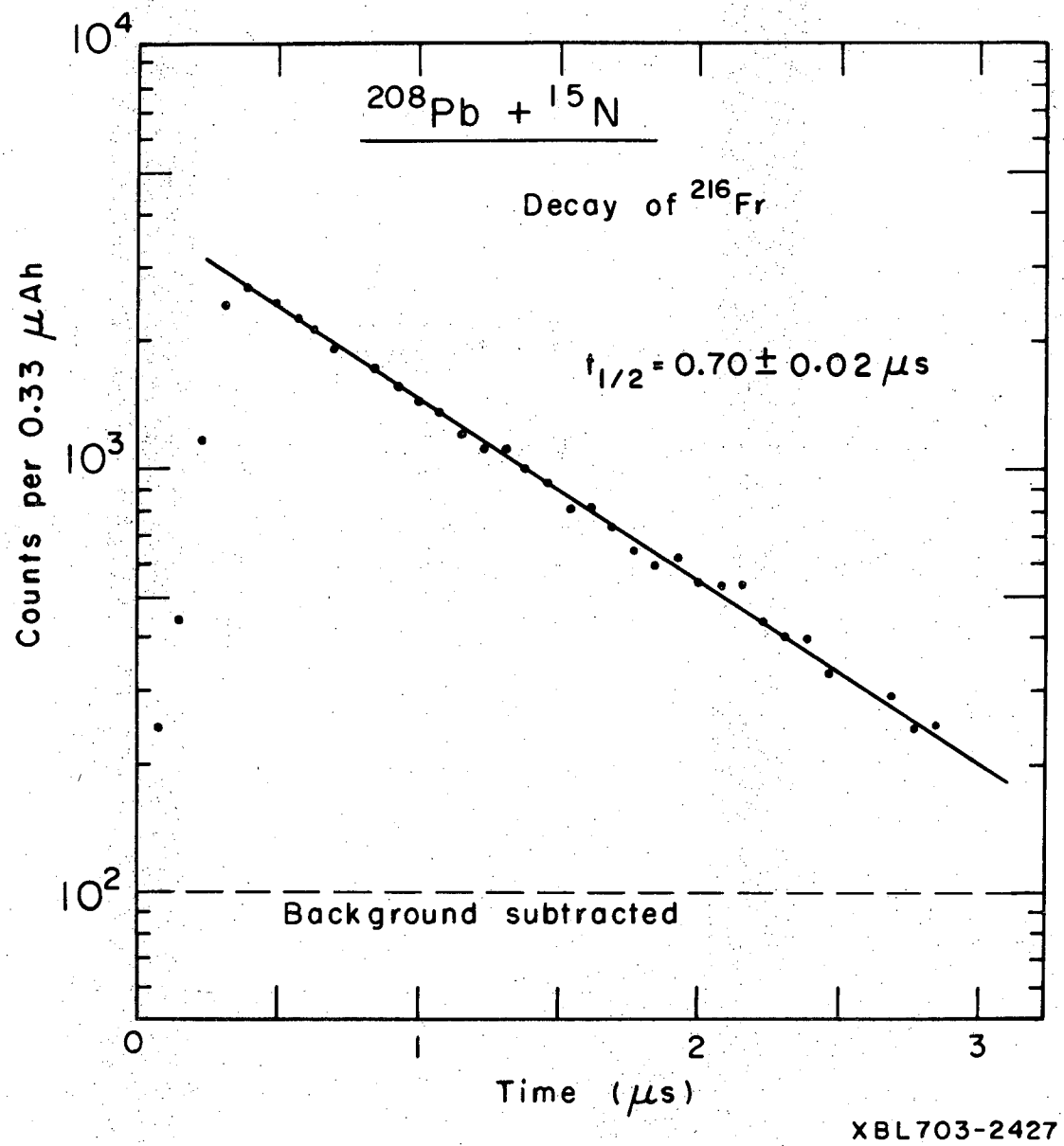
$^{208}Pb + ^{15}N$
Decay of ^{216}Fr
$t_{1/2} = 0.70 \pm 0.02\ \mu s$
Background subtracted
Counts per 0.33 μAh
10^4
10^3
10^2
0
1
2
3
Time (μs)
XBL703-2427

Fig. 20

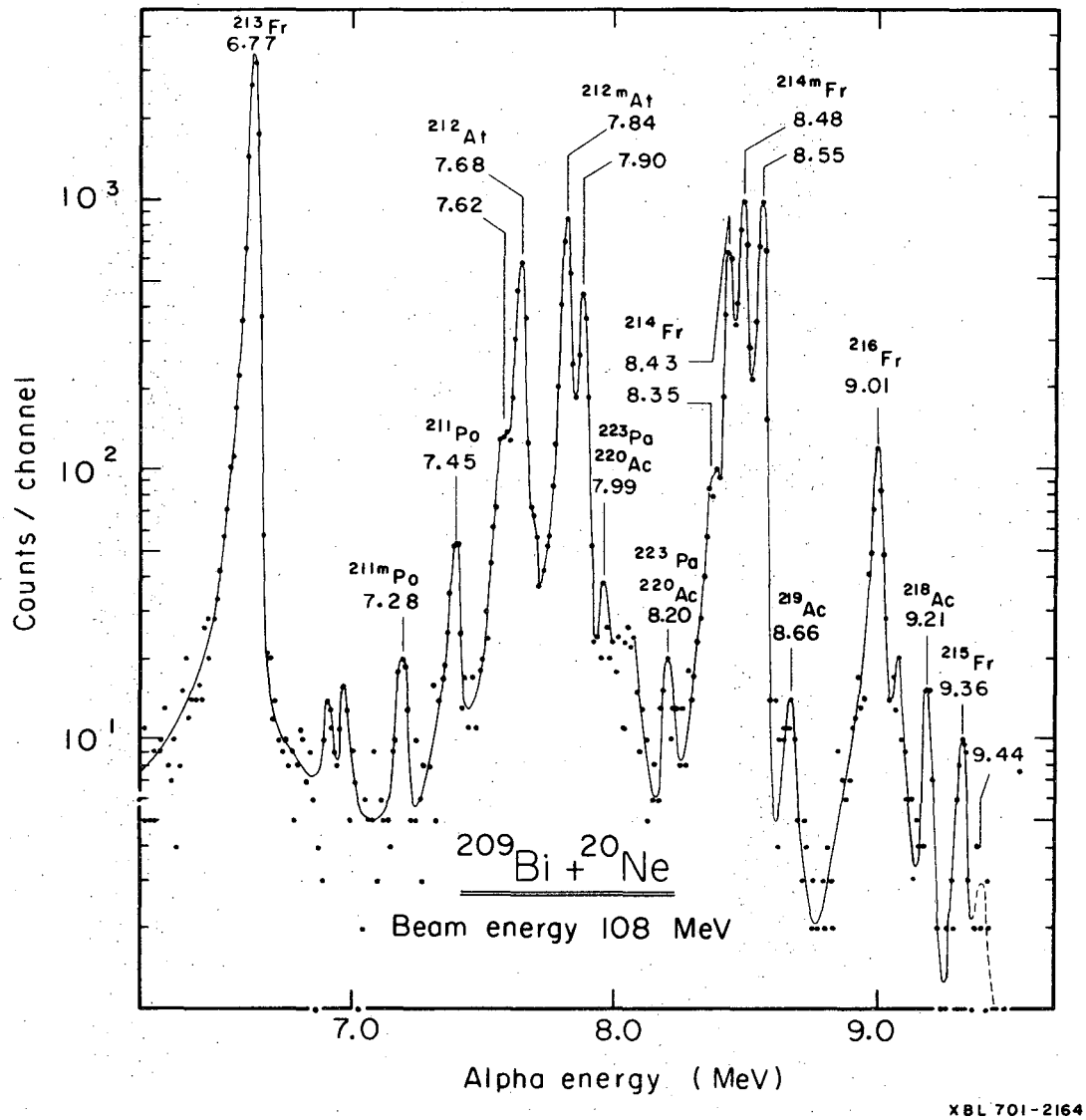
213Fr
6.77
212At
7.68
7.62
212mAt
7.84
7.90
214mFr
8.48
8.55
214Fr
8.43
8.35
216Fr
9.01
211Po
7.45
223Pa
220Ac
7.99
211mPo
7.28
223Pa
220Ac
8.20
219Ac
8.66
218Ac
9.21
215Fr
9.36
9.44
209Bi + 20Ne
Beam energy 108 MeV
Counts / channel
10 3
10 2
10 1
7.0
8.0
9.0
Alpha energy (MeV)
XBL 701-2164

Fig. 21

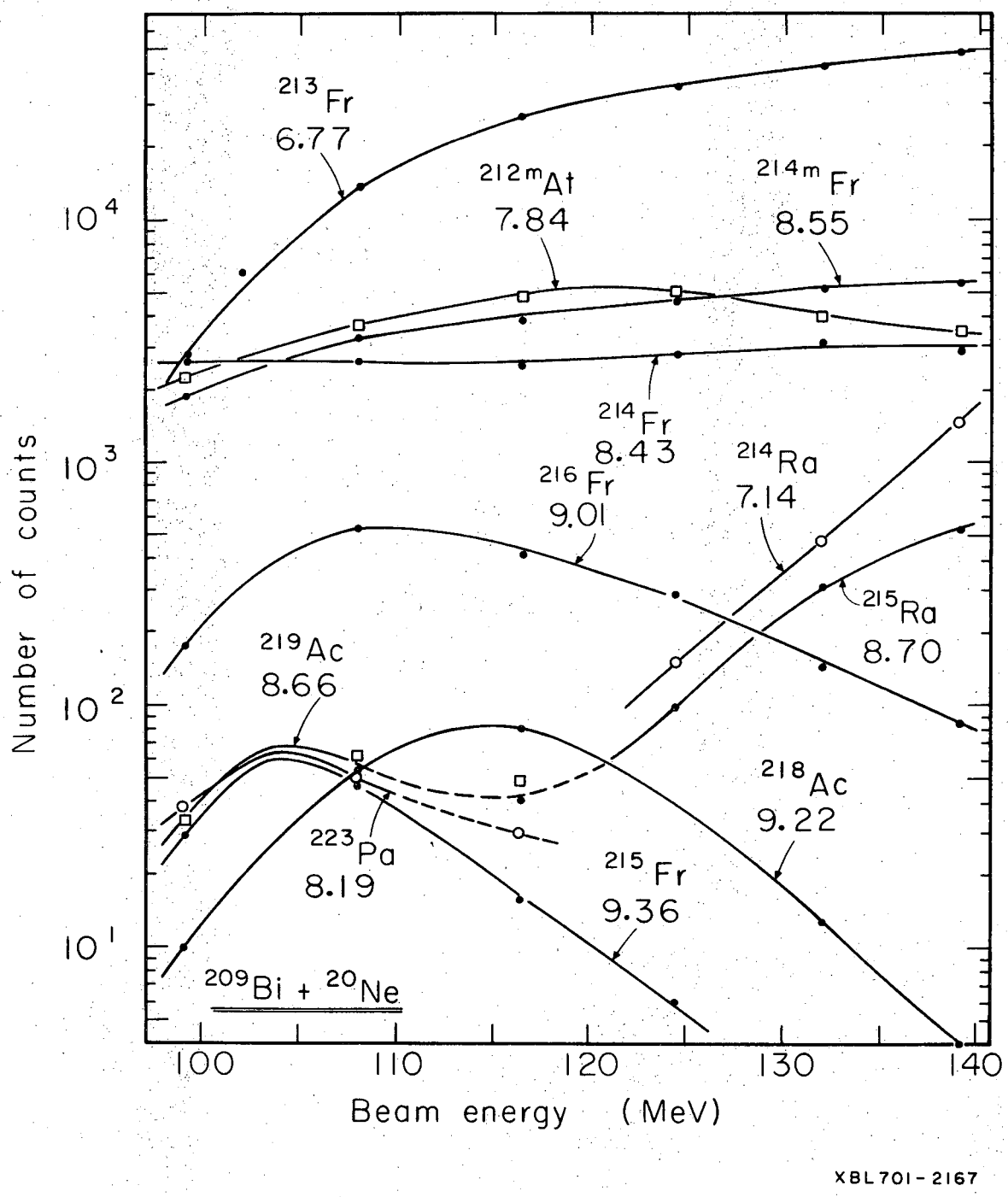
213 Fr
6.77
212m At
7.84
214m Fr
8.55
214 Fr
8.43
216 Fr
9.01
214 Ra
7.14
215 Ra
8.70
219 Ac
8.66
223 Pa
8.19
218 Ac
9.22
215 Fr
9.36
209 Bi + 20 Ne
Number of counts
10 4
10 3
10 2
10 1
100
110
120
130
140
Beam energy (MeV)
XBL701-2167

Fig. 22

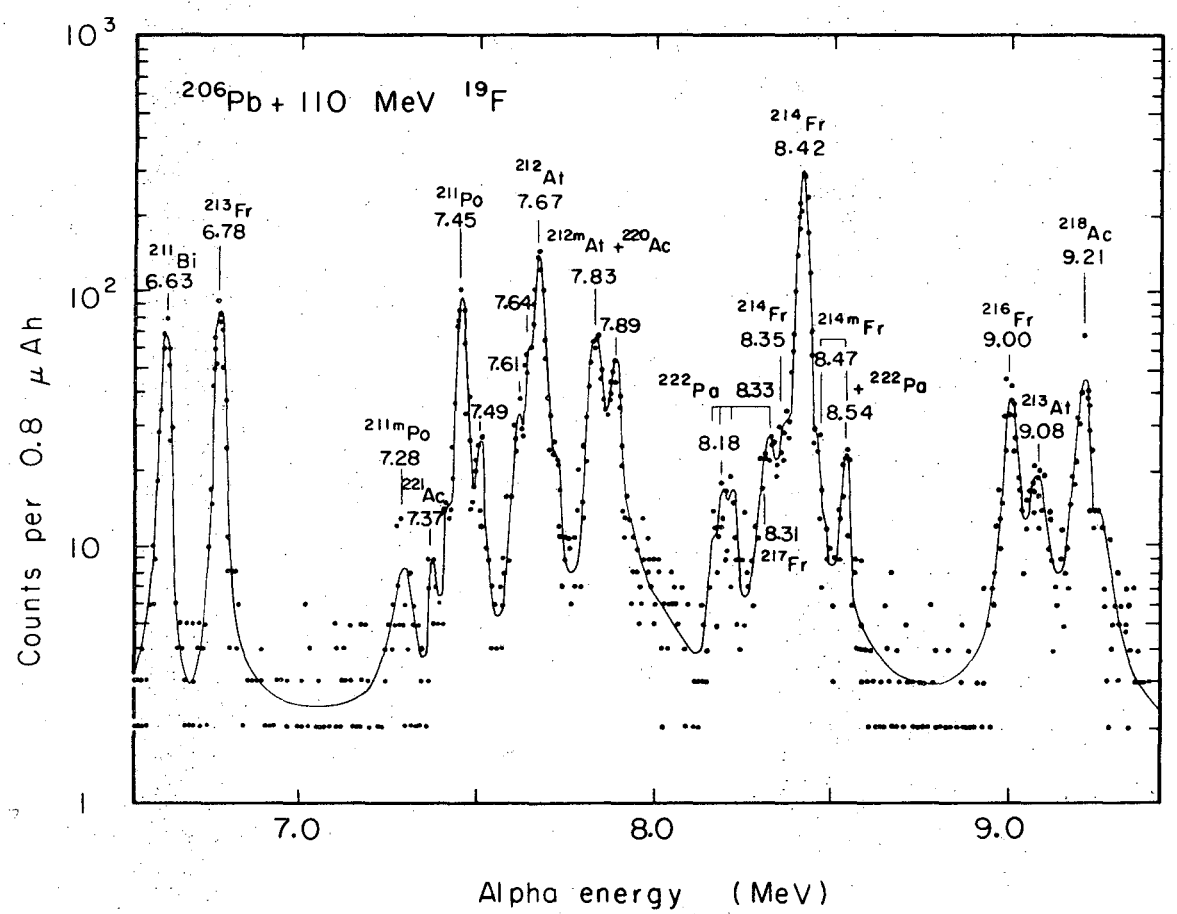
^{206}Pb + 110 MeV ^{19}F
^{211}Bi 6.63
^{213}Fr 6.78
^{211}Po 7.45
^{212}At 7.67
^{212m}At + ^{220}Ac 7.83
7.64
7.61
7.49
7.89
^{211m}Po 7.28
^{221}Ac 7.37
^{222}Pa 8.33
8.18
8.31
^{217}Fr
^{214}Fr 8.42
^{214}Fr 8.35
^{214m}Fr 8.47
+ ^{222}Pa 8.54
^{216}Fr 9.00
^{213}At 9.08
^{218}Ac 9.21
Counts per 0.8 μAh
Alpha energy (MeV)
XBL701-2241

Fig. 23

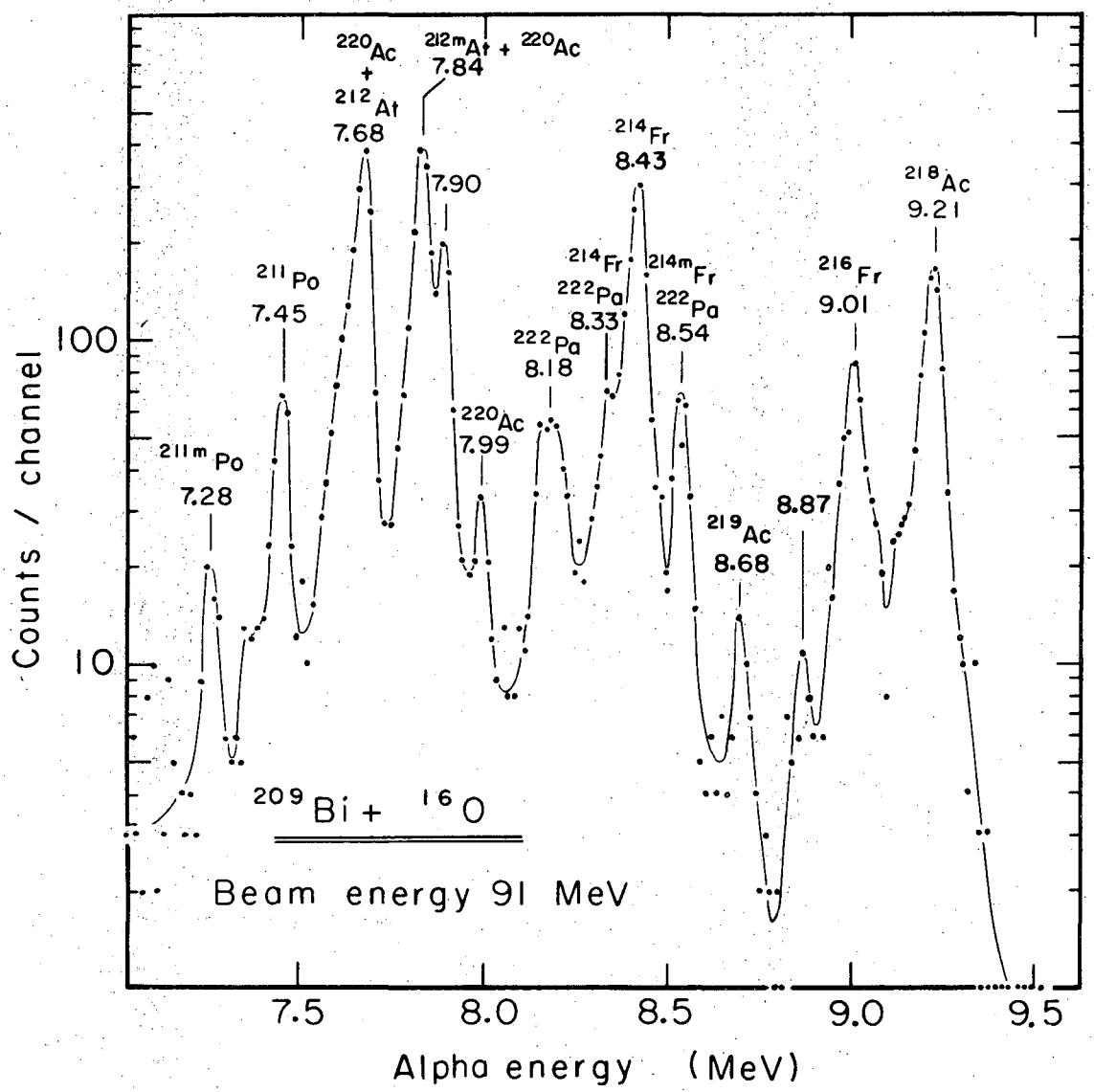

XBL701-2158

Fig. 24

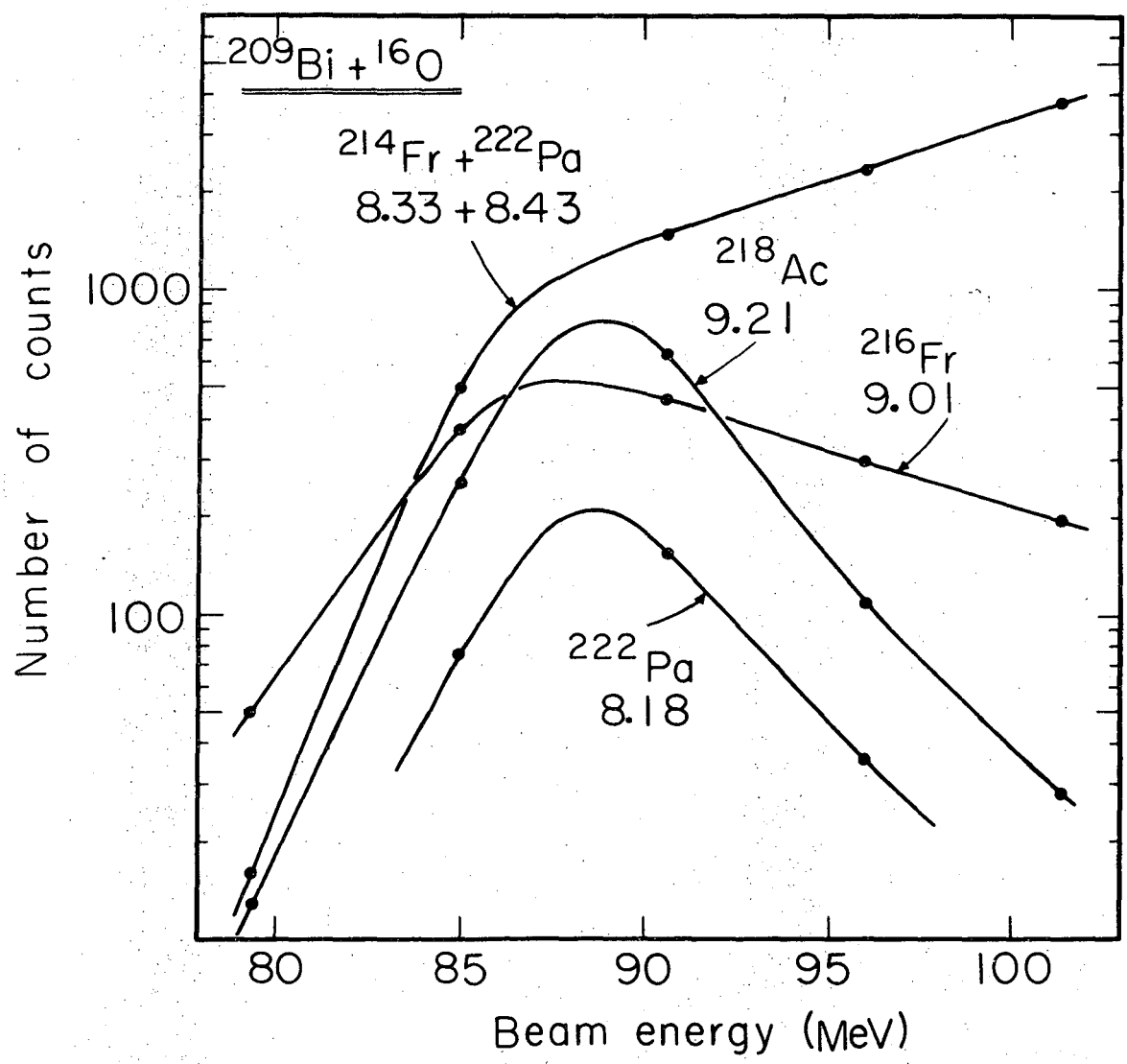

XBL701 - 2159

Fig. 25

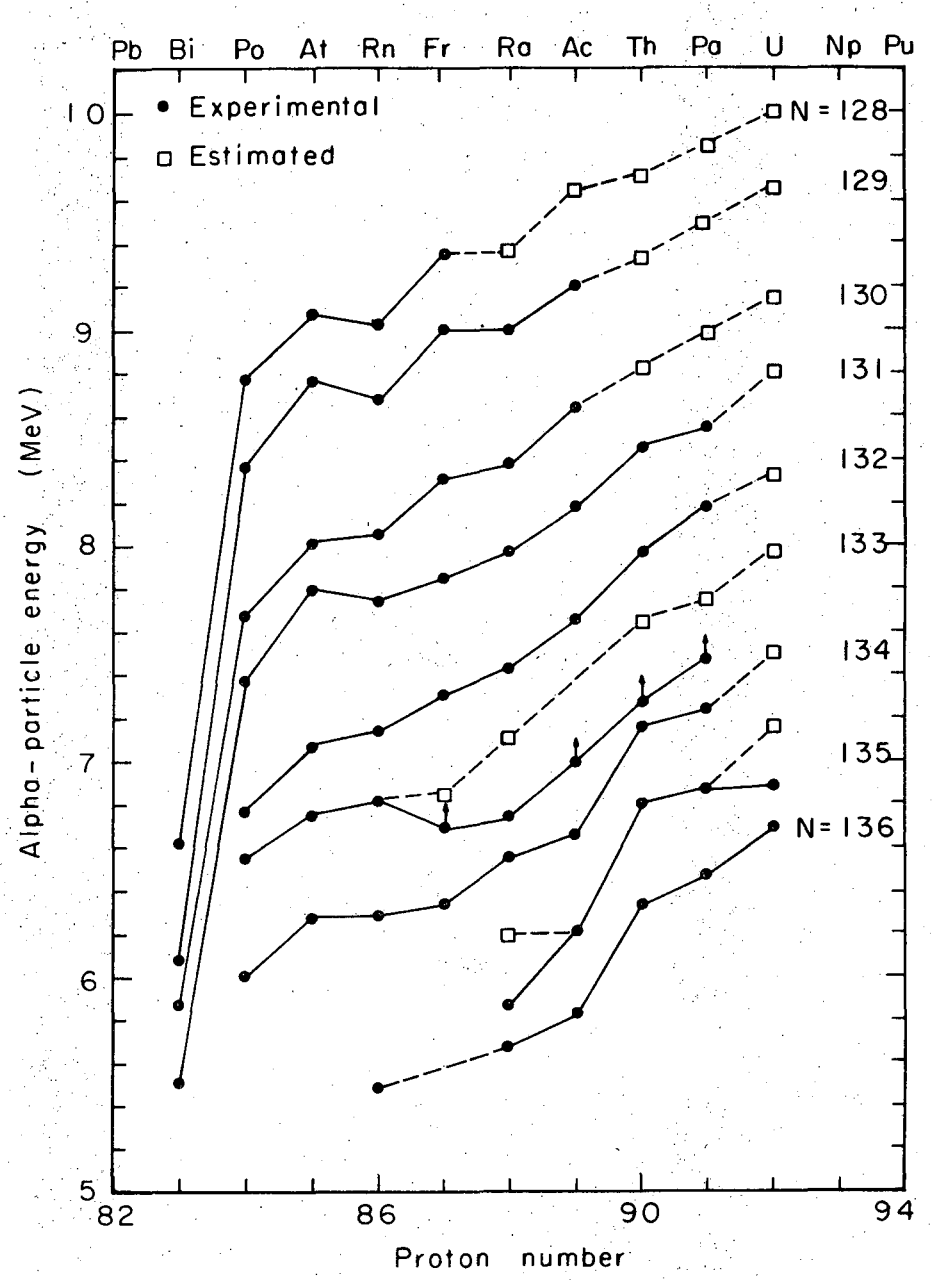

XBL701-2264

Fig. 26

LEGAL NOTICE

This report was prepared as an account of Government sponsored work. Neither the United States, nor the Commission, nor any person acting on behalf of the Commission:

A. Makes any warranty or representation, expressed or implied, with respect to the accuracy, completeness, or usefulness of the information contained in this report, or that the use of any information, apparatus, method, or process disclosed in this report may not infringe privately owned rights; or

B. Assumes any liabilities with respect to the use of, or for damages resulting from the use of any information, apparatus, method, or process disclosed in this report.

As used in the above, "person acting on behalf of the Commission" includes any employee or contractor of the Commission, or employee of such contractor, to the extent that such employee or contractor of the Commission, or employee of such contractor prepares, disseminates, or provides access to, any information pursuant to his employment or contract with the Commission, or his employment with such contractor.

TECHNICAL INFORMATION DIVISION
LAWRENCE RADIATION LABORATORY
UNIVERSITY OF CALIFORNIA
BERKELEY, CALIFORNIA 94720